THE JOURNAL OF BIOLOGICAL CHEMISTRY VOL. 284, NO. 21, pp. 14414–14427, May 22, 2009
Printed in the U.S.A.

# WISP1, a Pro-mitogenic, Pro-survival Factor, Mediates Tumor Necrosis Factor-α (TNF-α)-stimulated Cardiac Fibroblast Proliferation but Inhibits TNF-α-induced Cardiomyocyte Death*

Received for publication, December 29, 2008, and in revised form, March 16, 2009 Published, JBC Papers in Press, April 1, 2009, DOI 10.1074/jbc.M809757200

**Kaliyamurthi Venkatachalam[‡], Balachandar Venkatesan[‡], Anthony J. Valente[§], Peter C. Melby[‡§], Sailesh Nandish[§], Jane E. B. Reusch[¶‖], Robert A. Clark[‡§], and Bysani Chandrasekar[‡§1]**

*From the [‡]Department of Veterans Affairs, South Texas Veterans Health Care System, and [§]Department of Medicine, The University of Texas Health Science Center, San Antonio, Texas 78229, the [¶]Division of Endocrinology, Metabolism, and Diabetes, Department of Medicine, University Colorado Health Sciences Center, Aurora, Colorado 80110, and the [‖]Veterans Affairs Research Service, Denver Veterans Affairs Medical Center, Denver, Colorado 80220*

**WNT1-inducible signaling pathway protein-1 (WISP1), a member of the CYR61/CTGF/Nov family of growth factors, can mediate cell growth, transformation, and survival. Previously we demonstrated that WISP1 is up-regulated in post-infarct heart, stimulates cardiac fibroblast proliferation, and is induced by the proinflammatory cytokine tumor necrosis factor-α (TNF-α). Here we investigated (i) the localization of TNF-α and WISP1 in post-infarct heart, (ii) the mechanism of TNF-α-mediated WISP1 induction in primary human cardiac fibroblasts (CF), (iii) the role of WISP1 in TNF-α-mediated CF proliferation and collagen production, and (iv) the effects of WISP1 on TNF-α-mediated cardiomyocyte death. TNF-α and WISP1 expressions were increased in the border zones and non-ischemic remote regions of the post-ischemic heart. In CF, TNF-α potently induced WISP1 expression in cyclic AMP response element-binding protein (CREB)-dependent manner. TNF-α induced CREB phosphorylation *in vitro* and DNA binding and reporter gene activities *in vivo*. TNF-α induced CREB activation via ERK1/2, and inhibition of ERK1/2 and CREB blunted TNF-α-mediated WISP1 induction. Most importantly, WISP1 knockdown attenuated TNF-α stimulated collagen production and CF proliferation. Furthermore, WISP1 attenuated TNF-α-mediated cardiomyocyte death, thus demonstrating pro-mitogenic and pro-survival effects for WISP1 in myocardial constituent cells. Our results suggest that a TNF-α/WISP1 signaling pathway may contribute to post-infarct cardiac remodeling, a condition characterized by fibrosis and progressive cardiomyocyte loss.**

Acute myocardial infarction (MI)[2] is a major cause of morbidity and mortality worldwide. After acute MI, the two principal determinants of patient outcome are myocardial infarct size and the extent of left ventricular (LV) remodeling (1–3). Infarct size is determined during the acute phase immediately post-MI. LV remodeling on the other hand is a continuous and maladaptive process characterized by progressive left ventricular hypertrophy, fibrosis, ventricular dilatation, and by the gradual deterioration of cardiac performance, leading ultimately to congestive heart failure (1–3).

Numerically, fibroblasts are the major cell type in the heart, but they constitute a smaller total volume compared with cardiomyocytes (4). Fibroblasts are associated primarily with modulation of extracellular matrix and tissue healing/repair (4–6). Fibroblasts secrete collagens, fibrillins, fibronectin, laminin, and matrix metalloproteinases and, thus, are responsible for the maintenance of connective tissue homeostasis (4–7). We and others have shown that primary cardiac fibroblasts also produce various cytokines, chemokines, and growth factors (4–6, 8, 9), which tightly regulate the physiological function of the cells. Under pathological conditions, however, where the expression of cytokines and growth factors is significantly altered, the fibroblasts can undergo differentiation, migration, and proliferation, resulting in pathological fibrosis because of excessive accumulation of collagens and other ECM proteins (4–6).

The six members of the CCN (**C**YR61/**C**TGF/**N**ov) family of growth factors (Cyr61 (cysteine-rich 61, CCN1), CTGF (connective tissue growth factor, CCN2), Nov (nephroblastoma-overexpressed, CCN3), WISP1 (WNT1-inducible signaling pathway protein-1, CCN4), WISP2 (CCN5), and WISP3 (CCN6)) are involved in a number of cellular processes, including adhesion, migration, and proliferation (10–12). Although their roles in angiogenesis and oncogenesis are well character-

* This work was supported in part by the Research Service of the Department of Veterans Affairs.

[1] To whom correspondence should be addressed: Medicine/Cardiology, The University of Texas Health Science Center, 7703 Floyd Curl Dr., San Antonio, TX 78229-3900. Tel.: 210-567-4598; Fax: 210-567-6960; E-mail: chandraseka@uthscsa.edu.

[2] The abbreviations used are: MI, myocardial infarction; CF, cardiac fibroblasts; CRE, cAMP response elements; CREB, CRE-binding protein; Cyr61, cysteine-rich protein 61; CTGF, connective tissue growth factor; Nov, nephroblastoma-overexpressed gene; CCN, Cyr61/CTGF/Nov; dn, dominant negative; ECM, extracellular matrix; EMSA, electrophoretic mobility shift assay; ELISA, enzyme-linked immunosorbent assay; ERK, extracellular signal-regulated kinase; FM, fibroblast media; GFP, green fluorescent protein; IκB, inhibitory κB; IKK, IκB kinase; JNK, c-Jun NH2-terminal kinase; LV, left ventricle; MEK, mitogen (extracellular)-activated kinase; MMP, matrix metalloproteinase; NF-κB, nuclear factor κB; NMVM, neonatal mouse ventricular myocytes; PDGF, platelet-derived growth factor; RT-qPCR, reverse transcriptase quantitative PCR; shRNA, short hairpin RNA; siRNA, small interference RNA; TCF/LEF, T-cell factor-lymphoid enhancer binding factor; TGF, transforming growth factor; TNF-α, tumor necrosis factor-α; TNFR, TNF receptor; WISP1, WNT1-inducible signaling pathway protein-1; m.o.i., multiplicity of infection; BSA, bovine serum albumin; MTT, (3-(4,5-dimethylthiazol-2-yl)-2,5-diphenyl-2H-tetrazolium bromide.

ized, with the exception of CTGF, their precise contribution to myocardial remodeling is unknown. Recently we demonstrated that whereas WISP1 is expressed in the heart at low basal levels, permanent occlusion of the left anterior descending coronary artery significantly up-regulates its expression in the non-ischemic myocardium (13). Furthermore, we have found that WISP1 exerts both pro-hypertrophic and pro-mitogenic effects *in vitro*, stimulating Akt-dependent cardiomyocyte growth, as well as collagen synthesis and fibroblast proliferation (13). Because cardiomyocyte hypertrophy and fibroblast proliferation play central roles in remodeling and WISP1 regulates these two critical processes, it is plausible that WISP1 also mediates cardiac remodeling after myocardial ischemia, infarction, and inflammation. However, the mechanisms involved in the induction and regulation of WISP1 under these conditions have not been well characterized.

The proinflammatory cytokine tumor necrosis factor (TNF)-$\alpha$ is expressed at low basal levels in the normal myocardium but is significantly up-regulated after infection, inflammation, and injury (14, 15). Although low levels are considered cytoprotective (16, 17), aberrant expression of TNF-$\alpha$ during myocardial ischemic injury and inflammation induces cardiomyocyte death, hypertrophy of surviving cardiomyocytes, contractile dysfunction, fibroblast proliferation, fibrosis, and adverse remodeling (14–17). TNF-$\alpha$ exerts its biological effects via two cell surface receptors, TNFR1 (55 kDa) and TNFR2 (75 kDa) (18). TNFR1, which is more abundantly expressed in the heart, appears to be the main signaling receptor for TNF-$\alpha$ and is implicated in transmitting its deleterious effects (18). On the other hand, signaling through TNFR2 appears to exert a protective effect in the heart (18, 19). Of note, all myocardial constituent cells, including fibroblasts, express both TNFR1 and TNFR2 and, therefore, are targets of TNF-$\alpha$.

We have recently demonstrated that TNF-$\alpha$ induces WISP1 expression in cardiomyocytes (13). However, neither its localization in post-infarct myocardium, its role in TNF-$\alpha$-mediated cardiac fibroblast (CF) proliferation and collagen production, nor its effects on TNF-$\alpha$-mediated cardiomyocyte death are known. Our results show that both TNF-$\alpha$ and WISP1 are localized in the border zone and the non-infarct remote region in post-infarct myocardium. Furthermore, TNF-$\alpha$ induces WISP1 expression in CF via a TNFR2/MEK1/ERK1/2/CREB pathway and stimulates fibroblast collagen production in part via WISP1. In addition, WISP1 exerts pro-survival effects in cardiomyocytes, antagonizing TNF-$\alpha$-mediated cardiomyocyte death. Collectively, these results indicate that WISP1 exerts pro-mitogenic and pro-survival effects in cardiac cell type-specific manner, and TNF-$\alpha$/WISP1 signaling may be an important contributing mechanism in post-infarct cardiac remodeling.

## EXPERIMENTAL PROCEDURES

*Materials*—Recombinant human TNF-$\alpha$ (210-TA-010), neutralizing antibodies against TNF-$\alpha$ (AF-210-NA), TNFR1 (mouse IgG1; MAB225), and TNFR2 (mouse $IgG_{2a}$; MAB226), normal goat IgG (AB-108-C), normal mouse IgG1 (MAB002). and normal mouse $IgG_{2a}$ (MAB003) were purchased from R & D Systems (Minneapolis, MN). We have previously reported the effectiveness of anti-TNF-$\alpha$ neutralizing antibodies (20, 21). Anti-CREB (#9197), phospho-CREB (Ser-133; #9198S), extracellular signal-regulated protein kinase (ERK1/2; #9102), phospho-ERK1/2 (#9101S), JNK (#9252), phospho-JNK (#9251), and lamin A/C antibodies were from Cell Signaling Technology, Inc. (Beverly, MA). Anti-p65 and IKK$\beta$ antibodies were from Santa Cruz Biotechnology, Inc. (Santa Cruz, CA). U0126 (MEK inhibitor, 10 $\mu$M in DMSO for 20 min), PD98059 (ERK1/2 inhibitor, 10 $\mu$M in DMSO for 1 h), SP600125 (JNK inhibitor; 10 $\mu$M in DMSO for 30 min), and DMSO were purchased from EMD Biosciences (San Diego, CA). $\alpha$-Tubulin polyclonal antibody and all other chemicals were purchased from Sigma-Aldrich.

*Mouse Model of MI*—All animal studies conformed to the Guide for the Care and Use of Laboratory Animals, published by the National Institutes of Health (22), and were approved by the Institutional Animal Care and Use Committee of the University of Texas Health Science Center at San Antonio. Male C57Bl/6 mice weighing ~25–30 g and age 3–4 months underwent permanent occlusion of the left anterior descending coronary artery for 1 day as previously described (13).

*Immunohistochemistry*—TNF-$\alpha$ and WISP1 protein expressions were localized by Immunohistochemistry as previously described (23). Twenty-four hours after MI, animals were sacrificed, and hearts were removed, fixed in 10% buffered formalin for 24 h, and then embedded in paraffin. Six micrometer-thick sections were used for immunohistochemistry. The following primary antibodies were used: rabbit polyclonal WISP1 (1:50; H-55, sc-25441, Santa Cruz Biotechnology) and TNF-$\alpha$ (1: 200; Pierce-Endogen, Rockford, IL). Mayer's hematoxylin (Fluka, Ronkonkoma, NY) was used as a counterstain. Specificity was controlled by substituting the primary antibody with rabbit preimmune serum.

*Cardiac Fibroblasts*—Primary human CF were purchased from ScienCell Research Laboratories (#6300; San Diego, CA) and maintained and characterized as we have detailed earlier (7, 22). CF were grown in fibroblast medium (FM) supplied by the manufacturer and supplemented with 2% fetal bovine serum, fibroblast growth supplement, and antibiotics (complete media). At 70% confluency, the complete media was replaced with FM containing 0.5% BSA. After overnight incubation (quiescent cells), TNF-$\alpha$ (10 ng/ml) was added and cultured for the indicated time periods. At the end of experimental period, culture supernatants were collected and snap-frozen. Cells were harvested, snap-frozen, and stored at −80 °C.

*RNA Interference and Adenoviral Vectors*—TNFR1 (#sc-29507), TNFR2 ((#sc-36689), and non-targeting siRNA (#sc-37007) were purchased from Santa Cruz Biotechnology. In addition to siRNA-mediated knockdown, TNFR2 expression was also targeted by an short hairpin RNA (shRNA) expression vector with the following sequence: 5′-GTT CTC CAA CAC GAC TTC ATC CAC GGA TA-3′ (HuSH 29-mer shRNA construct, catalogue number TR308733, OriGene Technologies, Inc., Rockville, MD). A corresponding plasmid with an shRNA cassette targeted against green fluorescent protein (GFP; TGA CCA CCC TGA CCT ACG GCG TGC AGT GC) served as a negative control. CF were transfected with the siRNA (100 nM) or the shRNA expression vector (1 $\mu$g) using a Nucleofection kit

(#VPI-1002, Amaxa Inc., Gaithersburg, MD). Among the five recommended programs, the T-16 program gave optimal transfection efficiency (38%) with only 9% cell death (24). After overnight incubation in medium containing 0.5% BSA, dead cells were removed, and the incubation was continued for an additional 36 h. CREB was targeted by specific siRNA (sense, 5′-UAC AGC UGG CUA ACA AUG GdTdT-3′). Knockdown of individual proteins was confirmed by immunoblotting. In addition, CREB was also targeted by transducing CF with recombinant adenovirus expressing dominant negative mutant forms of CREB (KCREB, MCREB) (25). Adenoviral GFP (50 m.o.i., Ad.CMV-GFP, #1060, Vector Biolabs, Philadelphia, PA) served as a control. NF-κB activation was targeted as previously described (7) using adenoviral transduction of dominant-negative (dn) IKKβ (Ad.dnIKKβ), dnp65 (Ad.dnp65), and phosphorylation-deficient IκB-α (S32A/S36A; Ad.dnIκB-α). Expressions of IKKβ (sense, 5′-AAGTACACAGTGACCG-TCGAC-3′; Ambion, Austin, TX) and p65 (sense, 5′-UAUAGC-CUCAGGGUACUCCAUCAUCAGC-3′) were also targeted by specific siRNA at 100 nM. siRNA that does not target any gene in the human genome (5′-CUCGGC GUUUCAUCUGUGGd-TdT-3′) served as a negative control. Knockdown of respective proteins at 48 h was confirmed by immunoblotting.

*Electrophoretic Mobility Shift Assay (EMSA), ELISA, and Reporter Assays*—CREB DNA binding activity in nuclear extracts was analyzed by EMSA (7, 24, 26) using labeled, double-stranded, gene-specific wild-type (sense, 5′-GGG TTT GTC CTT CAC CCT **GAC GTC** AGA TCT TGC TTT AAT AAA ACC-3′) and mutant (sense, 5′-GGG TTT GTC CTT CAC CCT **GAA TTC** AGA TCT TGC TTT AAT AAA ACC-3′) oligonucleotides. Activation of CREB was also analyzed by ELISA (TransAM™ Transcription Factor ELISA kits; CREB (#42096), pCREB (#43096); Active Motif, Carlsbad, CA) using nuclear protein extracts (7, 24, 26). Activation of CREB was confirmed by reporter gene assays using adenoviral CRE-luciferase vector (Ad.CRE-Luc, 50 m.o.i., #1672, Vector Biolabs). The empty adenoviral construct (Ad.MCS-Luc, 50 m.o.i.; Vector Biolabs) served as a base-line control. Ad.β-gal (50 m.o.i.; Vector Biolabs) served as an internal control. β-Galactosidase activity in cell extracts was determined using a Luminescent β-Gal Detection Kit II (BD Biosciences), and the results are expressed in relative light units as a ratio of firefly luciferase to β-galactosidase activity.

Formation of NF-κB protein-DNA complexes in TNF-α-treated CF was analyzed by EMSA using double-stranded labeled NF-κB consensus (sense, 5′-AGTTGAGGGGACTTTCCCAG-GC-3) oligonucleotides (Santa Cruz Biotechnology). Specificity of NF-κB DNA binding activity was determined by competition with unlabeled consensus or mutant (sense, 5′-AGTTGAGGCGACT-TTCCCAGGC-3) NF-κB oligonucleotides.

*Chromatin Immunoprecipitation Assay*—CF were cultured in complete medium in 100-mm dishes until 70% confluent. The medium was replaced with FM plus 0.5% BSA and incubated overnight. TNF-α was added at the indicated doses and incubated for 2 h. The cells were then fixed by the addition of 280 μl of 37% formaldehyde (Sigma-Aldrich) to 10 ml of culture medium for 10 min at 37 °C, harvested, and processed for immunoprecipitation using a commercially available kit (chromatin immunoprecipitation assay kit, #17-295; Upstate Biotechnology Inc., Lake Placid, NY) and following the manufacturer's protocol (21). Immune complexes were eluted, the cross-linking was reversed using 5 M NaCl, and the DNA was isolated by phenol/chloroform extraction and ethanol precipitation. The final DNA pellet was dissolved in Tris-EDTA buffer. The supernatant from an immunoprecipitation carried out in the absence of c-Fos antibody was purified and used for the total input DNA control. The supernatant DNA was diluted 1:100 before PCR analysis. PCR was carried out on 1 μl of each sample using sense primer, 5′-TGG AGG TGG GGA CAG AGG-3′, and antisense primer, 5′-GGA TCC GAC CAC CTC TCG-3′, which amplified a 208-bp segment of the human *WISP1* gene from −250 to −42 relative to the translational start site. PCR products were analyzed on 2% agarose gels. Primers from the WISP1 open reading frame (GenBank™ accession# NM_003882; sense, 5′-AGG TGG TTC CTG CCC TGG AC-3′; antisense, 5′-CAC TCA CAG CCA TCT GTG AT-3′) that amplifies a 221-bp fragment were used in a control PCR.

*WISP1 Promoter-Reporter Assays*—A *WISP1* promoter reporter construct spanning the region from −328 to −39 bp relative to the translation start site (pWISP328) and containing a CREB site located at −328 bp (27) was amplified from human genomic DNA using the sense primer 5′-aag ctt CAC CCT AGT GTG AAG TCA TAG-3′ and the antisense primer 5′-gga tcc GGA TCC AGA GGA TCC GAC CAC CTC G-3′, cloned into the pCR2.1-TOPO vector, and sequence-verified. The sense primer contained a HindIII restriction site at the 5′ end, and the antisense primer contained a SacI site (lowercase). The insert was excised with HindIII and SacI and subcloned into the promoter/enhancer-less luciferase vector pGL3-Basic.

*Site-directed Mutagenesis*—Mutation of the CREB binding site in the *WISP1* promoter-reporter vector was performed by site-directed mutagenesis (21) using the QuikChange kit (Stratagene) with the following primers: sense, 5′-GTC CTT CAC CCT GAA TTC AGA TCT TGC TTT AAT A-3′. The mutation (TGACGTCA 224 TGAATTCA) was confirmed by nucleotide sequencing. pGL3-Basic served as a vector control.

*mRNA Expression Northern Blotting and Quantitative Real Time PCR (RT-qPCR)*—DNA-free total RNA was extracted using RNAqueous®-4PCR kit (Ambion). RNA quality was assessed by capillary electrophoresis using the Agilent 2100 Bioanalyzer (Agilent Technologies, Palo Alto, CA). All RNA samples used for quantitative PCR had RNA Integrity Numbers greater than 9.1 (scale = 1–10), as assigned by default parameters of the Expert 2100 Bioanalyzer software package (Version 2.02). Northern blot analysis was carried out as previously described (28) using 20 μg of total RNA. Membranes were probed with a $^{32}$P-labeled cDNA fragment. WISP1 and MMP1 cDNA were amplified by RT-PCR (WISP1, sense, 5′-GTG TGT GTA GGC AGG GAG TG-3′, and antisense, 5′-AGC ATG CAG AGT GTG CAG AG-3′; MMP1 (sense, 5′-ATT CTA CTG ATA TCG GGG CTT TGA-3′, and antisense, 5′-ATG TCC TTG GGG TAT CCG TGT AG-3′), subcloned into pCR 2.1-TOPO vector (Invitrogen), amplified, digested with EcoR1, and used for labeling. 28 S rRNA served as an internal control. Data for mRNA expression are shown as the ratio of signals

obtained for the specific gene to that of the corresponding 28 S rRNA.

WISP1 mRNA expression was confirmed by RT-qPCR using the primers 5′-AGA GCC GC CTC TGC AAC TT-3′ and 5′-GGA GAA GCC AAG CCC ATC A-3′. Actin (5′-GAT CAT TGC TCC TCC TGA GC-3′ and 5′-ACT CCT GCT TGC TGA TCC AC-3′) served as a control. cDNA was prepared by oligo(dT) priming (Ambion), and qPCR was carried out using the SYBR® green reporter molecule (Applied Biosystems, Foster City, CA), and an ABI Prism 7000 sequence detector (Applied Biosystems). The comparative cycle threshold method was used to analyze the data by generating relative values of the amount of target cDNA. MMP9 expression (sense, 5′-CACT-GTCCACCCCTCAGAGC-3′; antisense, 5′-GCCACTTGTC-GGCGATAGG-3′), analyzed similarly, was represented as fold difference in *MMP-9* gene expression relative to the actin.

*Analysis of Protein Expression Immunoblotting and ELISA*—Extraction of whole cell and nuclear protein, immunoblotting, autoradiography, and densitometry were performed as described previously (7, 13, 24). Briefly, CF were solubilized with Nonidet P-40 lysis buffer (0.5% Nonidet P-40, 10 mM Tris-HCl, pH 7.4, 150 mM NaCl, 3 mM *p*-amidinophenylmethanesulfonyl fluoride, 5 mg/ml aprotinin, 2 mM sodium orthovanadate, 5 mM EDTA). Samples were separated by 10% SDS-PAGE, transferred to polyvinylidene difluoride membrane, and probed with primary antibodies diluted in 2% nonfat dry milk in Tris-buffered saline containing 0.05% Tween 20 (TTBS) overnight at 4 °C. The blots were rinsed in TTBS for 30 min and then incubated in horseradish peroxidase-conjugated secondary antibodies in 5% milk in TTBS for 1 h and developed using a chemiluminescent substrate (SuperSignal Pico West + 5% SuperSignal Femto, Pierce).

*Immunocomplex Kinase Assays*—ERK1/2 activity was determined in whole cell homogenates using a colorimetric assay kit (ERK, p44/42 MAP Kinase Assay kit; Cell Signaling Technology, Inc.) (9, 26).

*Cell Proliferation and DNA Synthesis*—The effect of TNF-$\alpha$ on CF proliferation was analyzed by CyQUANT™ assay according to the manufacturer's protocol (Invitrogen (13, 29)). Briefly, second-passage CF were plated at 3000 cells per well into 96-well clear bottom, black-sided plates (VWR Scientific Products, West Chester, PA) and allowed to attach overnight. After 24 h, the cells were fed with serum-free medium containing 0.5% BSA and incubated for an additional 24 h. Cells were then continuously stimulated with TNF-$\alpha$ (1 ng/ml) or phosphate-buffered saline vehicle (controls) in serum-free medium for 72 h. After removing the medium, the plates were frozen at −80 °C for 2 h before assay. Plates were then thawed, stained with CyQUANT™ GR dye according to manufacturer's protocol (Molecular Probes, Eugene, OR), and assayed on a FLX800 microplate fluorescence reader (Bio-Tek Instruments, Winooski, VT) using 485/20 excitation and 528/20 emission filters, and analyzed using KC4 software (Bio-Tek).

Cell proliferation was also determined by $^3$H-thymidine ([$^3$H]TdR) incorporation. CF were plated at a concentration of 3000 cells/well in 200 $\mu$l of FM + 10% FBS in 96-well flat-bottom plates (Costar, Corning, NY). After 24 h incubation the complete medium was replaced with FM+0.5% BSA and incubated for an additional 24 h. The cells were treated with TNF-$\alpha$ (1 ng/ml) for the 72 h and were pulsed with 0.5 $\mu$Ci/well [$^3$H]TdR for the last 16 h of the incubation period. Cells were then harvested onto membranes, and the incorporated [$^3$H]TdR was measured in triplicate using a liquid scintillation counter (Beckman LS6500).

To demonstrate that TNF-$\alpha$-mediated CF proliferation is mediated by WISP1, CF were transfected with WISP1-specific shRNA expression vector. Among the four shRNA constructs supplied (#TR300454, OriGene Technology), the #TI301810 construct with the sequence ATGGCACAGGAACTGCAT-AGCTACACAA gave the best knockdown and was used in the present investigation. A purified and sequence-verified plasmid containing a non-effective 29-mer short hairpin GFP cassette (pRS-shGFP, #TR30003) served as a negative control. CF were co-transfected with *Renilla* luciferase vector to control for transfection efficiency (100 ng, pRL-TK). At 70% confluency, CF were transfected with the expression vectors using the Nucleofection kit (#VPI-1002) provided by Amaxa (Gaithersburg, MD) as we described above. After overnight culture in medium containing 0.5% BSA, dead cells were removed. The cells were then incubated with fresh medium for an additional 36 h followed by incubation with TNF-$\alpha$ for 3 days.

*Sircol Collagen Assay*—The effect of TNF-$\alpha$ on collagen expression by CF was determined as previously described using the Sircol collagen assay (Biocolor, Newtownabbey, N. Ireland) (13, 29, 30), which is based on the specific binding of the anionic dye Sirus red to the basic amino acid residues of collagen. Briefly, second-passage CF were plated into 100-mm culture dishes at 80% confluency, allowed to attach overnight, and refed the following day with serum-free medium containing 0.5% BSA. After 24 h CF were stimulated with TNF-$\alpha$ or phosphate-buffered saline vehicle in serum-free medium for 72 h. Levels of soluble collagens released into culture media were determined spectrophotometrically according to the manufacturer's instructions. Each collagen assay included standard curves using purified soluble collagen supplied by the manufacturer. To determine the role of WISP1 in TNF-$\alpha$-induced collagen expression, WISP1 expression was targeted using specific shRNA. 48 h after transfection with the shRNA, cells were treated with TNF-$\alpha$ for an additional 3 days. Levels of soluble collagens released into culture media were determined as before. Results were normalized to cell numbers and are presented as -fold induction from untreated.

*Assay of Collagenase-sensitive [$^3$H]Proline Incorporation*—Collagenase-sensitive [$^3$H]proline incorporation was determined essentially as described by Liu *et al.* (31). In brief, CF were seeded into 12-well plates in complete media, and after 16 h the media were replaced with media containing 0.5% BSA. 24 h later the quiescent CF were treated with TNF-$\alpha$ and 1 $\mu$Ci/well of [$^3$H]proline (PerkinElmer Life Sciences) for an additional 24 h. The cells were then treated overnight with 20% trichloroacetic acid. Precipitates were collected by centrifugation and washed 3 times with 1.0 ml of 5% trichloroacetic acid + 0.01% proline. Pellets were dissolved in 0.2 M NaOH, and the solutions were titrated to neutral pH with 0.2 M HCl. Collagenase (2 mg/ml; Worthington Biochemical Corp.) in Tris/$CaCl_2$/*N*-ethylmaleimide buffer was added to each tube, and samples

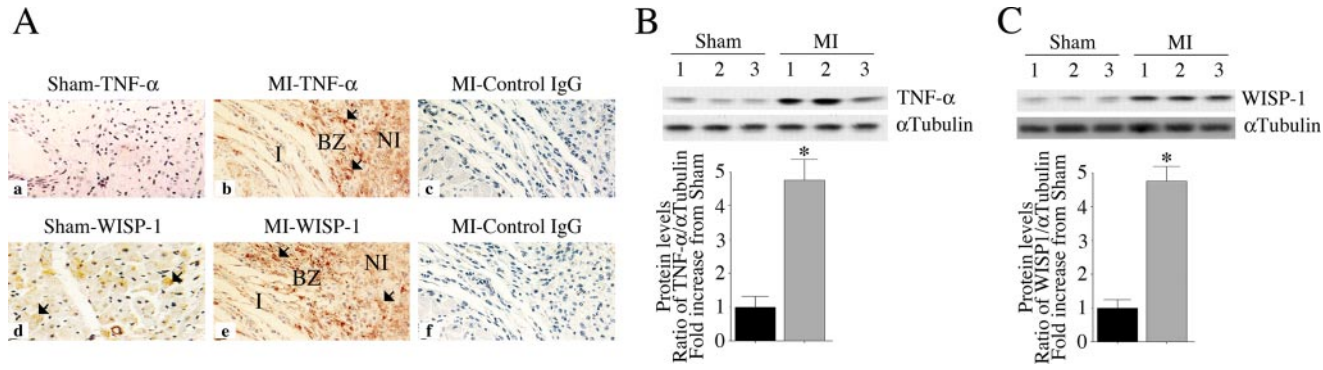


FIGURE 1. **Myocardial infarction up-regulates TNF-α and WISP1.** *A*, immunohistochemical localization of TNF-α and WISP1 in sham-operated and post-infarct myocardium. C57Bl/6 mice ($n = 3$/group) underwent permanent left anterior descending coronary artery ligation for 24 h. Sham-operated animals served as controls. Paraffin-embedded heart tissue was sectioned, deparaffinized, rehydrated, and used for localization of TNF-α (*a*, *b*, and *c*) and WISP1 (*d*, *e*, and *f*) by immunohistochemistry in sham (*a* and *d*) and MI (*b*, *c*, *e*, and *f*) hearts. Replacing primary antibody with preimmune sera served as controls (*c*, TNF-α; *f*, WISP1). *Arrows* denote specific immunoreactivity. *I*, infarct zone; *BZ*, border zone; *NI*, non-infarcted region. *B*, TNF-α protein levels in non-infarcted remote zone ($n = 3$; densitometric analysis from three independent experiments is summarized in the *lower panel*). Each lane represents 20 μg of protein extract from an individual animal. α-Tubulin served as a loading control. *, $p < 0.01$ *versus* Sham. *C*, WISP1 protein levels in non-infarcted remote zone ($n = 3$; densitometric analysis from three independent experiments is summarized in the *lower panel*). α-Tubulin served as a loading control. *, $p < 0.01$ *versus* Sham.

were allowed to incubate for 1 h at 37 °C. Samples were then placed on ice, and proteins were precipitated with 10% trichloroacetic acid for 1 h. Samples were centrifuged at 14,000 rpm for 10 min, and the collagenase-sensitive [$^3$H]proline in the supernatant was determined by liquid scintillation counting. Results were normalized to cell numbers and are presented as -fold induction from untreated.

*Cell Death ELISA*—To investigate whether the pharmacological inhibitor siRNA- or shRNA-mediated knockdown and adenoviral transduction of dominant negative expression vectors modulate cell viability, we analyzed cell death using an ELISA that quantifies mono- and oligo-nucleosomal fragmented DNA in the cytoplasmic fraction of cell lysates (Cell Death Detection ELISA$^{PLUS}$ kit; Roche Applied Science).

*Isolation of Neonatal Mouse Ventricular Cardiomyocytes (NMVM)*—To investigate whether WISP1 antagonizes TNF-α-mediated cardiomyocyte death, we treated NMVM with TNF-α for 24 h. NMVM were isolated from 1–3-day-old neonatal mice (C57Bl/6 background) by modifying a previously published protocol for the isolation of neonatal rat ventricular myocytes (32). To exclude non-muscle cells, the isolated cells were allowed to adhere to a tissue culture dish for 2 h at 37 °C, and the non-adherent cells (non-muscle cells adhere more rapidly) were collected and plated at a density of $1.0 \times 10^5$ cells/cm$^2$. Myocyte purity, determined by immunostaining for cardiac-sarcomeric actin (Sigma-Aldrich), averaged 94 ± 5%. 24 h after plating, NMVM were treated with WISP1 (0.1–100 ng/ml recombinant human WISP1, PeproTech, Rocky Hill, NJ) for 1 h before TNF-α addition (10 ng/ml). Twenty-four hours later, cell death was analyzed by Cell Death Detection ELISA$^{PLUS}$ kit.

*Cell Proliferation by the (3-(4,5-Dimethylthiazol-2-yl)-2,5-diphenyl-2H-tetrazolium Bromide (MTT) Colorimetric Assay*—Apoptotic cell death was also determined using a colorimetric assay kit based on the uptake of MTT by viable cells (Cell Proliferation kit; Roche Applied Science). The assay value obtained for vehicle treatment was considered as 100%. Complete inhibition in MTT reduction after exposure to 10% Triton X-100 is considered as 0%.

*Data Analysis*—Results are expressed as means ± S.E. For statistical analysis we used analysis of variance followed by an appropriate post hoc multiple comparison test (Tukey method). Data were considered statistically significant at $p < 0.05$.

## RESULTS

*Localization of TNF-α and WISP1 in Post-infarct Myocardium*—We and others have demonstrated that TNF-α (33) and WISP1 (13) are induced after myocardial infarction. Our previous studies showed that the WISP1 protein is significantly increased in the heart 24 h after MI (13). In the current study we performed immunohistochemistry to localize TNF-α and WISP1 expressions in the myocardium post-infarct. Sham-operated animals at 24 h served as controls. At this time point only low to undetectable levels of TNF-α could be observed in sham-operated animals (Fig. 1*Aa*). However, 24 h after induction of MI, increased levels of TNF-α protein were found. These were localized to the border zone and non-infarct left ventricular tissue areas. Immunoreactive TNF-α was detected mainly in cardiomyocytes and cardiac fibroblasts (Fig. 1*Ab*). Replacing the primary antibody with preimmune serum abolished the signals (Fig. 1*Ac*), demonstrating specificity of the TNF-α immunostaining. Increased levels of TNF-α were confirmed by immunoblotting. Significantly higher levels of TNF-α were seen in the extracts of the non-ischemic remote region tissue compared with the sham-operated controls (Fig. 1*B*). In contrast to TNF-α, detectable levels of WISP1 were observed in the myocardium of the sham-operated animals (Fig. 1*Ad*). However, after MI (Fig. 1*Ae*) WISP1 expression was increased in the border zone as well as in the non-infarcted remote region and, as with TNF-α, was localized mainly to cardiomyocytes and fibroblasts. No staining was seen with the preimmune serum control (Fig. 1, *Af*). Immunoblotting confirmed the significantly increased levels of WISP1 in the non-ischemic remote regions of the heart (Fig. 1*C*). Together, these results demonstrate that MI increases both TNF-α and WISP1 expression in the heart,

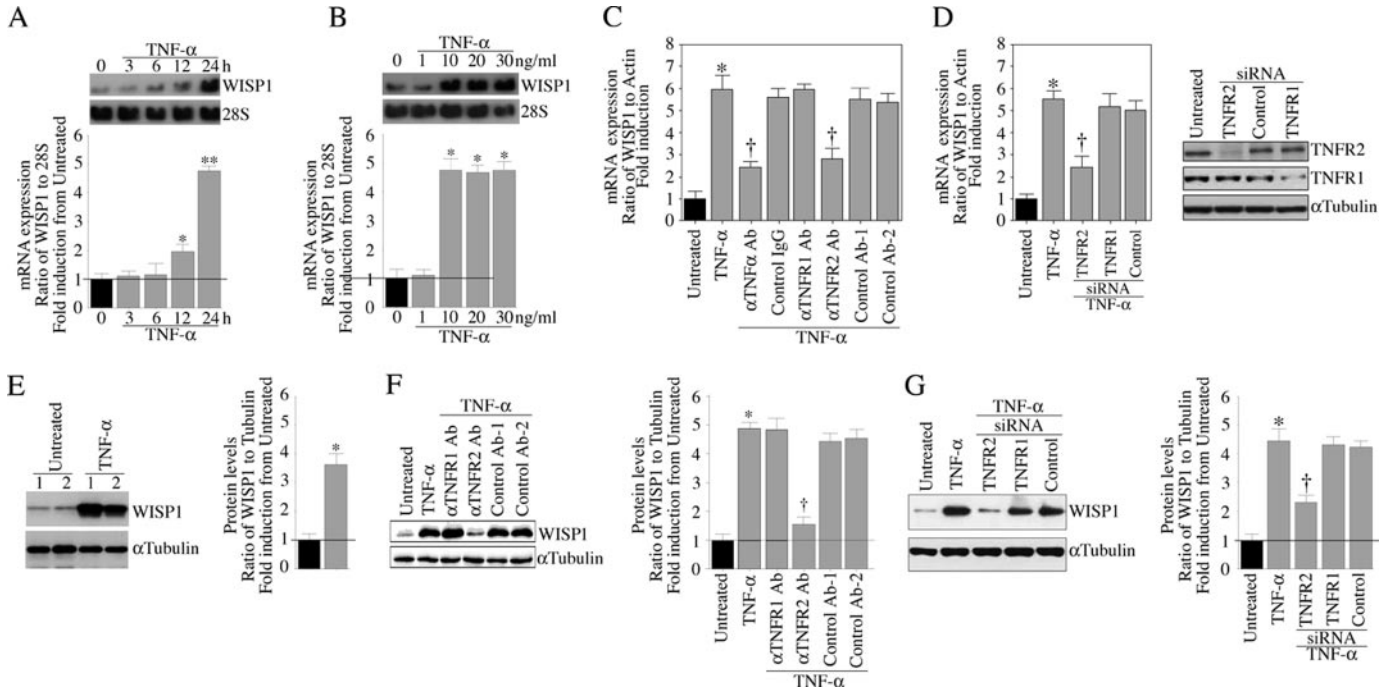


FIGURE 2. **TNF-α induces WISP1 expression in primary human cardiac fibroblasts.** *A*, TNF-α induces WISP1 mRNA in a time-dependent manner. Quiescent CF were treated with recombinant human TNF-α (10 ng/ml). Total RNA isolated at the indicated times was assayed for WISP1 mRNA expression by Northern blot analysis. 28 S rRNA served as an internal control. Autoradiographic bands were analyzed by video image densitometry, and results from three independent experiments are summarized in the *lower panel*. *, $p < 0.05$; **, $p < 0.001$ *versus* untreated. *B*, quiescent CF were treated with increasing concentrations of TNF-α for 24 h. WISP1 mRNA expression was analyzed as in *A*. *, $p < 0.001$ *versus* untreated. *C*, TNF-α induces WISP1 mRNA expression via TNFR2. Quiescent CF were incubated with anti-TNF-α- or TNFR-specific neutralizing antibodies (*Ab*, 10 μg/ml for 1 h) before the addition of TNF-α. WISP1 mRNA expression was analyzed by RT-qPCR ($n = 3$). Actin served as an internal control. *, $p < 0.001$ *versus* untreated; †, $p < 0.01$ *versus* the respective control antibody. *D*, TNFR2 knockdown attenuates TNF-α mediated WISP1 expression. CF were treated with TNFR-specific siRNA (100 nM for 48 h) before the addition of TNF-α (10 ng/ml for 24 h). WISP1 mRNA was quantified by RT-qPCR. Knockdown of TNFRs was confirmed by immunoblotting (*right panel*). *, $p < 0.001$ *versus* untreated; **, $p < 0.01$ *versus* TNF-α. *E*, TNF-α induces WISP1 protein expression. CF treated as in *A*, but for 24 h, were analyzed for WISP1 protein levels by immunoblotting. α-Tubulin served as an internal control. Densitometric analysis from three independent experiments is summarized in the *right panel*. *, $p < 0.001$ *versus* untreated. *F*, TNF-α induces WISP1 protein expression via TNFR2. CF treated as in *C* were analyzed for WISP1 protein by immunoblotting ($n = 3$). α-Tubulin served as an internal control. Densitometric analysis from three independent experiments is summarized in the *right panel*. *, $p < 0.001$ *versus* untreated; †, $p < 0.001$ *versus* respective control antibody. *G*, TNFR2 knockdown attenuates TNF-α-mediated WISP1 protein expression. CF treated as in *D* were analyzed for WISP1 protein by immunoblotting. Densitometric analysis from three independent experiments is summarized in the *right panel*. *, $p < 0.001$ *versus* untreated; †, $p < 0.05$ *versus* the respective control siRNA.

and this increased expression is localized to the same region of the post-infarct myocardium (Fig. 1).

*TNF-α Induces WISP1 Expression in Human Primary Cardiac Fibroblasts*—TNF-α plays a major role in post-infarct cardiac remodeling (34–37), a condition characterized by fibroblast proliferation and fibrosis. TNF-α has been shown to induce fibroblast proliferation (38, 39) via mechanisms that are not completely known. We hypothesized that TNF-α induces WISP1 expression in cardiac fibroblasts and stimulates their proliferation in a WISP1-dependent manner. In cultured CF, TNF-α stimulated WISP1 mRNA expression in a time- and dose-dependent manner (Fig. 2, *A* and *B*), with peak levels observed at 24 h (~5-fold, $p < 0.001$ *versus* untreated; Fig. 2*A*, results from three independent experiments are summarized in the *lower panel*) and with 10 ng/ml TNF-α (4.89-fold, $p < 0.001$ *versus* untreated; results from three independent experiments are summarized in the lower panel). Furthermore, TNF-α did not induce CF death, even at 30 ng/ml for 24 h (data not shown).

TNF-α signals via two different ubiquitously expressed cell surface receptors, p55 (TNFR1) and p75 (TNFR2). Binding of TNF-α to these receptors activates distinct intracellular signal transduction pathways. Although signaling via TNFR1 exerts pro-apoptotic effects (18), binding to TNFR2, which lacks the cytoplasm death domain and is, thus, unable to recruit FADD (Fas-associated protein with death domain), activates pro-survival effects (19). Therefore, to determine the receptor specificity in TNF-α-mediated WISP1 induction, CF were incubated with receptor-specific neutralizing antibodies before the addition of TNF-α. Neutralization of TNFR2, but not TNFR1, significantly attenuated TNF-α-mediated WISP1 induction (Fig. 2*C*, $p < 0.01$ *versus* TNF-α, $n = 3$). The respective normal mouse $IgG_{2a}$ and IgG1 controls failed to modulate TNF-α-mediated WISP1 expression. The specificity of TNFR2 in TNF-α signaling was further confirmed by incubating CF with receptor-specific siRNA. Knockdown of TNFR2, but not TNFR1, significantly attenuated TNF-α-mediated WISP1 induction (Fig. 2*D*; knockdown of respective proteins was confirmed by immunoblotting, as shown in the *right panel*). An siRNA that does not target any gene in the human genome served as a control and failed to modulate TNF-α-mediated WISP1 expression (Fig. 2*D*).

Having demonstrated that TNF-α induces WISP1 mRNA expression in CF (Fig. 2*A*), we next investigated whether TNF-α up-regulates WISP1 protein levels. Consistent with our data on mRNA expression (Fig. 2*A*), treatment of CF resulted in a robust increase in WISP1 protein levels at 24 h (3.78-fold, Fig.

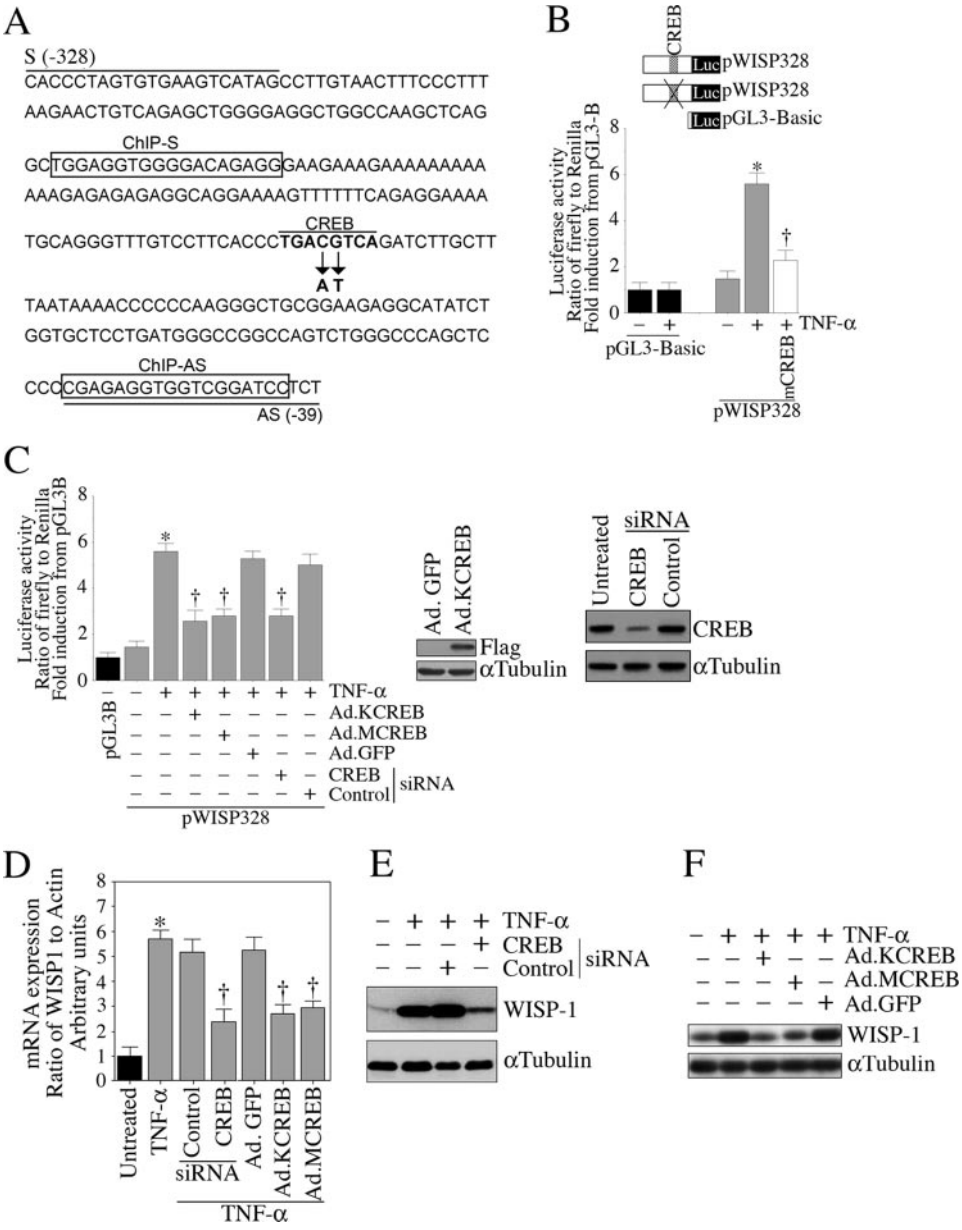


FIGURE 3. **TNF-α induces WISP1 expression via CREB.** *A*, WISP1 promoter sequence (−39 to −328 bp) with CREB binding site (pWISP328) and corresponding mutation in the CREB core sequence indicated. Primer sequences used to amplify the 5′ *cis* regulatory region (*underlined*) and in the chromatin immunoprecipitation assay (*boxed*) are also shown. *B*, TNF-α induction of WISP1 promoter-reporter activity is CREB-dependent. CF were transiently transfected with wild type or mutant WISP1 promoter-reporter constructs (schema shown in the *upper panel*) or empty vector (pGL3-Basic) before TNF-α addition. *Renilla* luciferase vector was co-transfected for a transfection efficiency control. Firefly and *Renilla* luciferase activities were determined after 12 h. *, $p < 0.001$ *versus* untreated; †, $p < 0.01$ TNF-α-treated WT *versus* TNF-α-treated mutant CREB. *C*, adenoviral transduction of mutant CREBs (FLAG-tagged KCREB; expression of FLAG is confirmed by immunoblotting and is shown in the *right panel*; and MCREB) or CREB knockdown attenuates TNF-α-induced WISP1 promoter-reporter activity. CF were transiently transfected with pWISP328 and CREB-specific siRNA (100 nM for 48 h; knockdown of CREB is confirmed by immunoblotting, and a representative of three independent experiments is shown in the *right panel*) or transduced with mutant CREBs. *Renilla* luciferase vector was used as the transfection control, and pGL3-Basic vector served as an internal control. Firefly and *Renilla* luciferase activities were determined after 12 h. *, $p < 0.001$ *versus* untreated; †, $p < 0.05$ *versus* TNF-α-treated pWISP328. *D*, adenoviral transduction of mutant CREBs or CREB knockdown blunts TNF-α-induced WISP1 mRNA expression. CF transfected as in *C* or treated with CREB siRNA were incubated with TNF-α for 24 h. WISP1 mRNA expression was analyzed by RT-qPCR. *, $p < 0.001$ *versus* untreated; †, $p <$ at least 0.05 *versus* TNF-α. *E*, knockdown of CREB or overexpression of mutant CREB (*F*) blunts TNF-α-induced WISP1 protein expression. CF treated as in *D* were analyzed for WISP1 protein expression by immunoblotting. Representatives of three independent experiments are shown.

2*E*; results from three independent experiments are summarized in the *right panel*), an effect that was significantly attenuated by TNFR2 but not TNFR1-neutralizing antibodies (Fig. 2*F*; results from three independent experiments are summarized in the *right panel*, 2.38-fold, $p < 0.001$ *versus* TNF-α + control IgG), and knockdown of TNFR2 (Fig. 2*G*; results from three independent experiments are summarized in the *right panel*; 1.89-fold, $p < 0.01$ *versus* TNF-α + control siRNA). Together, these results demonstrate that TNF-α induces WISP1 expression in primary cardiac fibroblasts via TNFR2 (Fig. 2).

*TNF-α Induces WISP1 Transcription via CREB*—We extended these studies to determine the mechanism of TNF-α-induced WISP1 expression in CF cells. The 5′ *cis*-regulatory region of *WISP1* has been cloned and characterized (27), and in addition to TCF/LEF binding sites, a CREB site (TGACGTCA) was identified that was shown to play a critical role in *WISP1* transcription. Because TNF-α is a potent inducer of CREB activation (40, 41), we investigated the effect of TNF-α on *WISP1* transcription. CF were transiently transfected with pWISP328, a *WISP1* promoter construct that contains the CREB site (Fig. 3*A*), and then treated with TNF-α. TNF-α stimulated *WISP1* promoter-reporter activity by at least 5.8-fold ($p < 0.001$ *versus* untreated, $n = 12$), a response that was significantly blunted when the core CREB binding site was mutated (TGAcgTCA 224 TGAatTCA; $p < 0.01$, $n = 12$). The empty pGL3-Basic vector, which served as a control, showed no changes in its low basal activity after TNF-α treatment. To confirm further the role of CREB in TNF-α regulation of WISP1, we targeted CREB expression by two different methods; that is, adenoviral transduction with dominant negative mutant CREB (Ad.KCREB and Ad.MCREB (25)) and knockdown using specific siRNA. Both adenoviral transduction of FLAG-tagged KCREB or MCREB (Fig. 3*C*, expression of KCREB was confirmed by immunoblotting for FLAG expression, and a representative of three independent experiments is shown on the *right*) and CREB knockdown (Fig. 3*C*; knockdown of CREB is shown in the *right panel*) significantly attenuated

TNF-α-dependent *WISP1* promoter-reporter activity (Fig. 3*C*), WISP1 mRNA expression (Fig. 3*D*), and protein levels (Fig. 3, *E* and *F*). Together, these results demonstrate that CREB is a key regulator of TNF-α-mediated WISP1 expression in cardiac fibroblasts (Fig. 3).

*TNF-α Activates CREB*—We have demonstrated that TNF-α induces *WISP1* transcription via CREB (Fig. 3). Because signal-dependent CREB activation results from Ser-133 phosphorylation (42), we investigated CREB activation by immunoblotting using activation-specific antibodies. Treatment with TNF-α increased CREB phosphorylation in a time-dependent manner (Fig. 4*A*). Densitometric analysis from three independent experiments, summarized in Fig. 4*B*, shows at least a 3.2-fold increase in phospho-CREB levels at 1 h after TNF-α addition. We next investigated CREB activation by EMSA using *WISP1* gene-specific primers. The low levels of CREB DNA binding activity, observed under basal conditions, showed a significant time-dependent increase after TNF-α treatment (Fig. 4*C*, 15 min, $p < 0.05$; 1 h, $p < 0.001$ *versus* untreated, $n = 3$). Furthermore, the reporter assays using adenoviral transduction of CRE-Luc vector (Fig. 4*D*) and ELISA (Fig. 4*E*) confirmed TNF-α-dependent CREB activation. Importantly, in chromatin immunoprecipitation assays we observed that treatment with TNF-α induced CREB binding *in vivo* to the *WISP1* promoter (Fig. 4*F*). Together, these results demonstrate CREB DNA binding both *in vitro* and *in vivo* in cardiac fibroblasts after TNF-α treatment (Fig. 4).

*TNF-α Induces WISP1 Expression via ERK1/2- but Not JNK-dependent CREB Activation*—Having demonstrated that TNF-α activates CREB via phosphorylation at Ser-133 (Fig. 4*A*) and knowing that TNF-α activates various downstream stress-activated protein kinases, including the ERK1/2 (43), we investigated whether ERK1/2 mediates TNF-α-induced CREB phosphorylation and WISP1 induction. TNF-α rapidly induced ERK1/2 phosphorylation (Fig. 5*A*, a representative of three independent experiments is shown) and increased its kinase activity in CF (Fig. 5*B*), effects that were inhibited by pretreatment with TNF-α neutralizing antibody, the MEK inhibitor U0126, or the ERK1/2 inhibitor PD98059 (Fig. 5*C*). Similarly, the MEK inhibitor U0126 as well as the ERK1/2 inhibitor PD98059, both, inhibited TNF-α-mediated CREB phosphorylation (Fig. 5*D*), CREB DNA binding activity (Fig. 5*E*), CRE reporter activity (Fig. 5*F*), and WISP1 mRNA expression (Fig. 5*G*). Furthermore, TNF-α induced JNK activation in CF as evidenced by an increase in phospho-JNK levels at 1 h, an effect that was significantly attenuated by pretreating CF with the JNK inhibitor SP600125 (Fig. 5*H*). However, pretreatment with SP600125 failed to modulate TNF-α-mediated CREB phosphorylation (Fig. 5*I*) and WISP1 mRNA expression (Fig. 5*J*). In contrast, SP600125 significantly inhibited TNF-α-mediated MMP1 expression (Fig. 5*K*). Furthermore, treatment with SP600125 did not affect CF viability (data not shown). Together, these results indicate that TNF-α induction of WISP1 expression is dependent on ERK1/2 activation of CREB but is independent of JNK (Fig. 5).

*TNF-α-mediated WISP1 Induction Is Independent of NF-κB*—TNF-α is a potent inducer of NF-κB in diverse cell systems (44). The ability of TNF-α to regulate cellular gene expression in most instances is attributed to activation of NF-κB-dependent signaling. Therefore, we investigated whether NF-κB plays a role in TNF-α-mediated WISP1 expression. Results in Fig. 6*A* show that TNF-α increased NF-κB DNA binding activity in CF,

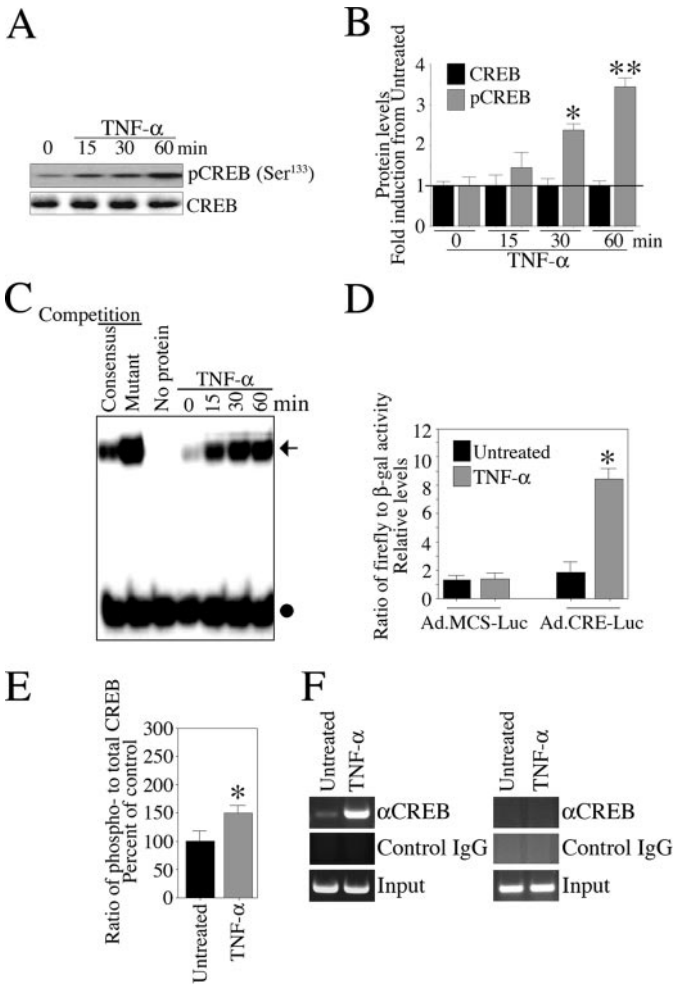


FIGURE 4. **TNF-α activates CREB.** *A*, TNF-α induces CREB phosphorylation. Quiescent CF were treated with TNF-α, and CREB activation was analyzed by immunoblotting using activation-specific antibodies and nuclear protein extracts. Total CREB served as a loading control. Densitometric analysis from three independent experiments is summarized in *panel B* and is shown as a ratio of pCREB to corresponding total CREB. *, $p < 0.01$; **, $p < 0.001$ *versus* the corresponding untreated. *C*, TNF-α induces CREB DNA binding activity. CF treated as in *A* were analyzed for CREB DNA binding activity by EMSA using the nuclear protein extracts. A representative of three independent experiments is shown. The *arrow* indicates specific DNA-protein complexes. The *solid circle* at the *bottom* denotes unincorporated labeled probe. *D*, TNF-α stimulates CRE-dependent reporter gene activity. Quiescent CF were transduced with Ad.CRE-Luc (50 m.o.i.). Ad.MCS-Luc (50 m.o.i.) served as a control. Ad.β-Gal (50 m.o.i.) served as an internal control. After 24 h cells were treated with TNF-α (10 ng/ml), and firefly luciferase and β-galactosidase activities were determined after 12 h ($n = 6$). *, $p < 0.001$ *versus* the corresponding untreated. *E*, activation of TNF-α-mediated CREB phosphorylation is confirmed by ELISA. CF treated as in *C* were analyzed for pCREB and total CREB by ELISA using nuclear protein extracts ($n = 12$). The results are expressed as a ratio of pCREB to corresponding total CREB and shown as percent of control. *, $p < 0.05$ *versus* untreated. *F*, chromatin immunoprecipitation analysis of the *WISP1* CREB binding site. Quiescent CF were treated with TNF-α for 1 h, and then cross-linked chromatin was prepared and immunoprecipitated with or without antibodies to CREB before amplification of the *WISP1* gene region containing the CREB site. No specific DNA was amplified in the chromatin immunoprecipitated with control antibody (*middle lanes* in *both panels*). Specific DNA sequences in the chromatin immunoprecipitated by CREB antibody are shown in the *upper left-hand panel*. Amplification of the input DNA is shown in the *bottom panels* ($n = 3$).

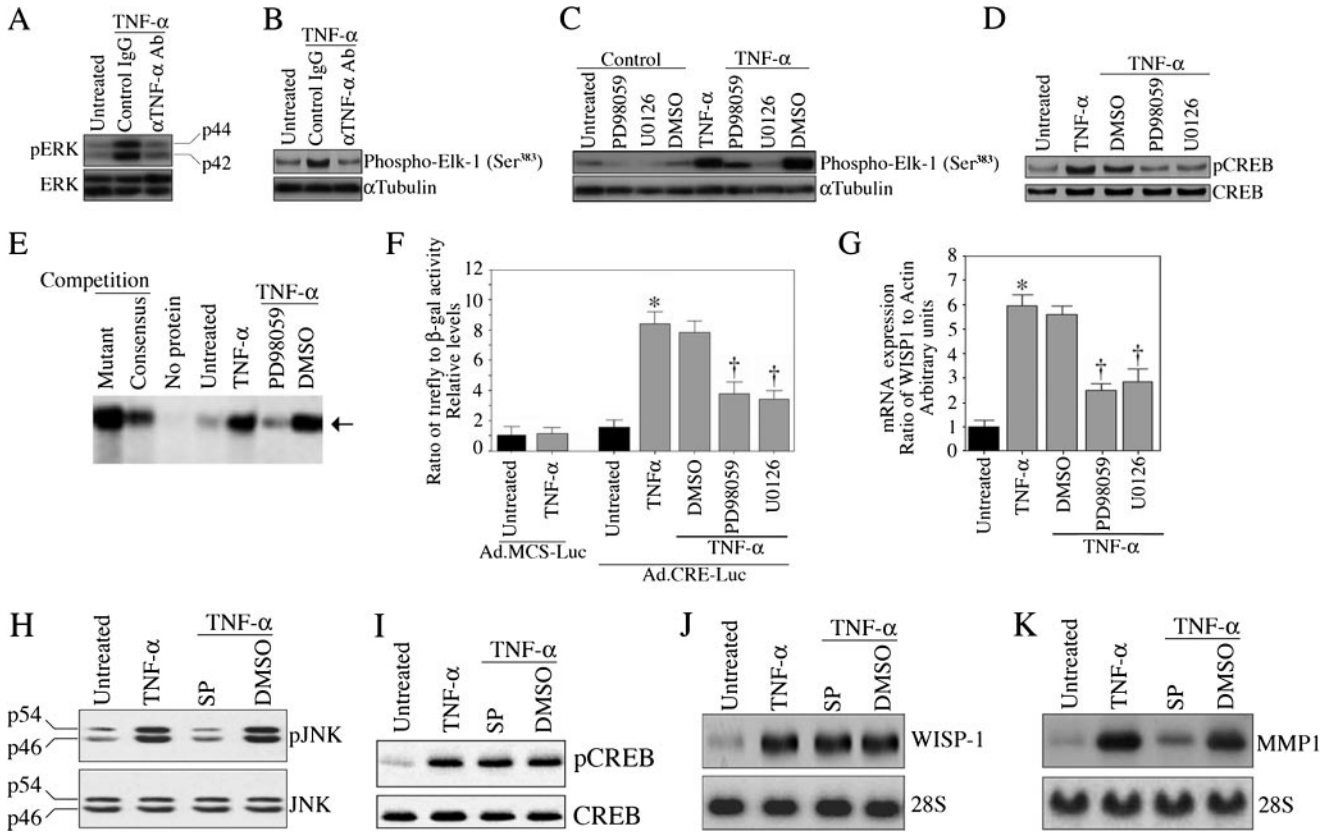


FIGURE 5. **TNF-α induces WISP1 expression via ERK1/2, but not JNK, activation.** *A*, TNF-α induces ERK1/2 phosphorylation. Quiescent CF were treated with TNF-α for 1 h. Total protein was extracted, and cleared cell lysates were analyzed for total and phospho-ERK1/2 by immunoblotting using activation-specific antibodies (*Ab*). Specificity of TNF-α was verified by preincubating the cells with TNF-α neutralizing antibodies before TNF-α addition. A representative of three independent experiments is shown. *B*, TNF-α stimulates ERK1/2 kinase activity. CF treated as in *A* were analyzed for ERK1/2 kinase activity using a commercially available colorimetric assay kit ($n = 3$). Elk-1 served as a substrate. *C*, TNF-α-induced ERK1/2 activity is blocked by PD (*PD98059*, 10 μM in DMSO for 1 h) and U0126 (10 μM in DMSO for 20 min). Quiescent CF were treated with the ERK1/2 and MEK inhibitors before TNF-α addition. ERK1/2 kinase activity was analyzed as in *B* ($n = 3$). *D*, TNF-α induces CREB phosphorylation via MEK and ERK1/2. Quiescent CF were treated with PD or U0126 before TNF-α addition. CREB activation was analyzed as in Fig. 4*A* ($n = 3$). *E*, TNF-α induces CREB DNA binding activity via ERK1/2. Quiescent CF were treated as in *D*, and CREB DNA binding activity in nuclear protein extracts was analyzed by EMSA ($n = 3$). The *arrow* indicates CREB-specific DNA-protein complexes. *F*, TNF-α induces CRE reporter gene activity via MEK and ERK1/2. Quiescent CF transduced with Ad.CRE-Luc as in Fig. 4*D* were treated with the MEK inhibitor U01226 or ERK1/2 inhibitor PD before TNF-α addition (10 ng/ml for 12 h). Ad.MCS-Luc served as a control. Ad.β-Gal served as an internal control. Firefly luciferase and β-galactosidase activities were determined as described under "Experimental Procedures" ($n = 6$). *, $p < 0.001$ *versus* the corresponding untreated. *G*, TNF-α induces WISP1 mRNA expression via MEK and ERK1/2. Quiescent CF treated as in *D* and *F*, but for 24 h, were analyzed for WISP1 mRNA expression by RT-qPCR ($n = 3$). *, $p < 0.001$ *versus* untreated; †, $p <$ at least 0.05 *versus* TNF-α. *H*, TNF-α induces JNK phosphorylation. Quiescent CF were treated as with the JNK inhibitor SP 600125 (*SP*) before TNF-α addition (10 ng/ml for 1 h). Total and phospho-JNK levels were analyzed in cleared cell lysates by immunoblotting using activation-specific antibodies ($n = 3$). *I*, inhibition of JNK fails to modulate TNF-α-induced CREB phosphorylation. Quiescent CF treated as in *H* were analyzed for total and phospho-CREB levels by immunoblotting ($n = 3$). *J*, inhibition of JNK fails to modulate TNF-α-mediated WISP1 expression. Quiescent CF treated as in *H*, but for 12 h, were analyzed for WISP1 mRNA expression by Northern blotting ($n = 3$). *J*, inhibition of JNK attenuates TNF-α-mediated MMP1 expression. Quiescent CF treated as in *J* were analyzed for MMP1 mRNA expression by Northern blotting ($n = 3$).

an effect that was attenuated by preincubating the cells with anti-TNF-α-neutralizing antibodies. Furthermore, adenoviral transduction of dominant negative IKKβ, IκB-α, and p65 or knockdown of IKKβ and p65 significantly attenuated TNF-α-mediated NF-κB activation (Fig. 6*B*). Knockdown of IKKβ and p65 was confirmed by immunoblotting (Fig. 6*C*). However, inhibition of NF-κB failed to significantly modulate TNF-α-mediated WISP1 expression (Fig. 6*D*). In contrast, inhibition of NF-κB significantly attenuated TNF-α-mediated MMP9 expression, and this reduction in MMP9 expression was not because of reduction in cell viability (Fig. 6*F*). These results demonstrate that although TNF-α can potently activate NF-κB in CF and induce NF-κB responsive genes such as *MMP9*, it most likely induces WISP1 expression via an NF-κB-independent pathway (Fig. 6).

*TNF-α Induces CF Proliferation and Collagen Synthesis via WISP1*—TNF-α has previously been shown to play a role in fibroblast proliferation *in vitro* (38, 39) and fibrosis *in vivo* after myocardial infarction. Because we have demonstrated robust induction of WISP1 after myocardial infarction (13) as well as potent induction of fibroblast proliferation by WISP1 (13), we investigated whether TNF-α treatment results in WISP1-dependent CF proliferation. Using both a CyQuant cell viability assay and [$^3$H]TdR incorporation into DNA, we found that TNF-α potently induced CF proliferation, an effect that was significantly attenuated by TNF-α- or TNFR2-neutralizing antibodies (Fig. 7*A*). Serving as respective controls, normal mouse $IgG_{2a}$ and IgG1 failed to inhibit TNF-α-induced CF proliferation. Furthermore, TNF-α induction of CF proliferation was significantly attenuated, although not abrogated, when

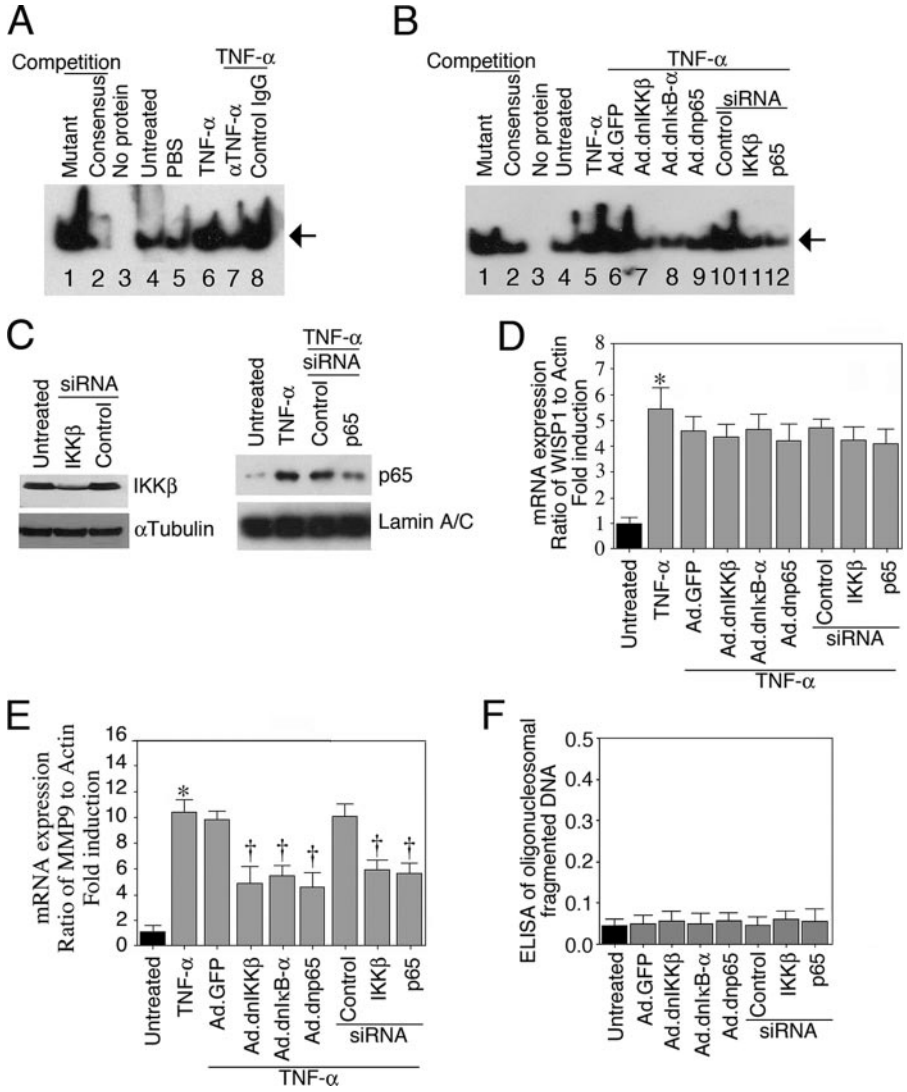


FIGURE 6. **TNF-α-mediated WISP1 expression is not dependent on NF-κB activation.** *A*, TNF-α stimulates NF-κB DNA binding activity. Quiescent CF were treated with TNF-α (10 ng/ml) for 1 h. Nuclear protein was extracted and analyzed for NF-κB DNA binding activity by EMSA ($n = 3$). Specificity of TNF-α was verified by incubating cells with TNF-α neutralizing antibodies (10 μg/ml for 1 h) before TNF-α addition. *Lanes 1* and *2*, control studies determining the specificity of NF-κB oligonucleotide was shown in the competition experiments. *Lane 3*, no nuclear protein but contains [γ-$^{32}$P]ATP-labeled κB-specific probe. *Arrow*, NF-κB-specific DNA-protein complexes. *PBS*, phosphate-buffered saline. *B*, adenoviral transduction of dnIKKβ, dnIκB-α, and dnp65 or siRNA-mediated IKKβ and p65 knockdown blunts TNF-α-mediated NF-κB DNA binding activity. CF were transfected with Ad.dnIKKβ, Ad.dnIκB-α, or Ad.dnp65 (100 m.o.i.) or transfected with IKKβ or p65 siRNA (100 nM for 48 h) before TNF-α addition ($n = 3$). Ad.GFP and non-targeting siRNA served as the respective controls. NF-κB DNA binding activity was analyzed by EMSA. The *arrow* indicates NF-κB-specific DNA-protein complexes. *C*, knockdown of IKKβ and p65 was confirmed by immunoblotting. *D*, inhibition of NF-κB fails to modulate TNF-α-induced WISP1 mRNA expression. CF treated as in *B* were incubated with TNF-α for 12 h. WISP1 mRNA expression was analyzed by RT-qPCR ($n = 6$). *E*, inhibition of NF-κB attenuates TNF-α-induced MMP9 expression. CF treated as in *D* were analyzed for MMP9 expression by RT-qPCR ($n = 6$). *F*, inhibition of NF-κB fails to affect CF viability. CF treated as in *B* were analyzed for cell death at 24 h by a cell death detection ELISA kit ($n = 6$).

WISP1 was targeted by specific shRNA (Fig. 7*B*; knockdown of WISP1 was confirmed by immunoblotting; *right panel*). Similarly, knockdown of WISP1 attenuated TNF-α-mediated DNA synthesis, as evidenced by a significant reduction in [$^3$H]TdR incorporation (Fig. 7*C*). Knockdown of WISP1, adenoviral transduction of mutant CREB, CREB knockdown, and inhibition of ERK1/2 by PD98059 all significantly attenuated TNF-α-induced CF proliferation (Fig. 7*D*) without affecting cell viability (Fig. 7*E*). Furthermore, knockdown of WISP1 attenuated [$^3$H]proline incorporation (Fig. 7*F*) and newly synthesized collagens (Fig. 7*G*). Together, these results demonstrate that TNF-α induces fibroblast proliferation and collagen synthesis in part via WISP1 (Fig. 7).

*WISP1 Attenuates TNF-α-mediated Cardiomyocyte Death*—Expression of TNF-α is elevated in myocardial injury and failure (14–17). Although it exerts pro-mitogenic effects in cardiac fibroblasts, sustained high levels of TNF-α induce cardiomyocyte death. Because WISP1 exerts pro-survival effects (45), we investigated whether WISP1 blocks TNF-α-mediated cardiomyocyte death. NMVM were pretreated with WISP1 before TNF-α addition, and cell death was analyzed by quantifying fragmented DNA in the cytoplasmic extracts. Results in Fig. 8*A* show that TNF-α induces significant cardiomyocyte death at 24 h and is attenuated by WISP1 in a dose-dependent manner, with maximal inhibition detected at 10 ng/ml. These results were further confirmed by the MTT cell viability assay (Fig. 8*B*). These results indicate that WISP1 can act as a pro-survival factor, attenuating TNF-α-induced cardiomyocyte death (Fig. 8).

## DISCUSSION

Our studies show that (i) both TNF-α and WISP1 are increased in the post-infarct myocardium, and this increased expression is localized to the same region of the heart, (ii) TNF-α induces WISP1 expression in cardiac fibroblasts via TNFR2/MEK1/ERK/CREB signaling, (iii) WISP1 mediates TNF-α-induced CF proliferation and collagen synthesis, and (iv) WISP1 can attenuate TNF-α-mediated cardiomyocyte death. Because TNF-α and WISP1 are up-regulated in the myocardium post-infarct and play critical roles in modulating fibroblast proliferation and cardiomyocyte survival, our results suggest that TNF-α/WISP1 signaling may contribute to post-infarct cardiac remodeling, a condition characterized by fibrosis and progressive cardiomyocyte loss (Fig. 8*C*).

Myocardial remodeling post-infarct and pressure overload are characterized by cardiomyocyte hypertrophy and fibrosis. Remodeling features increased turnover and deposition

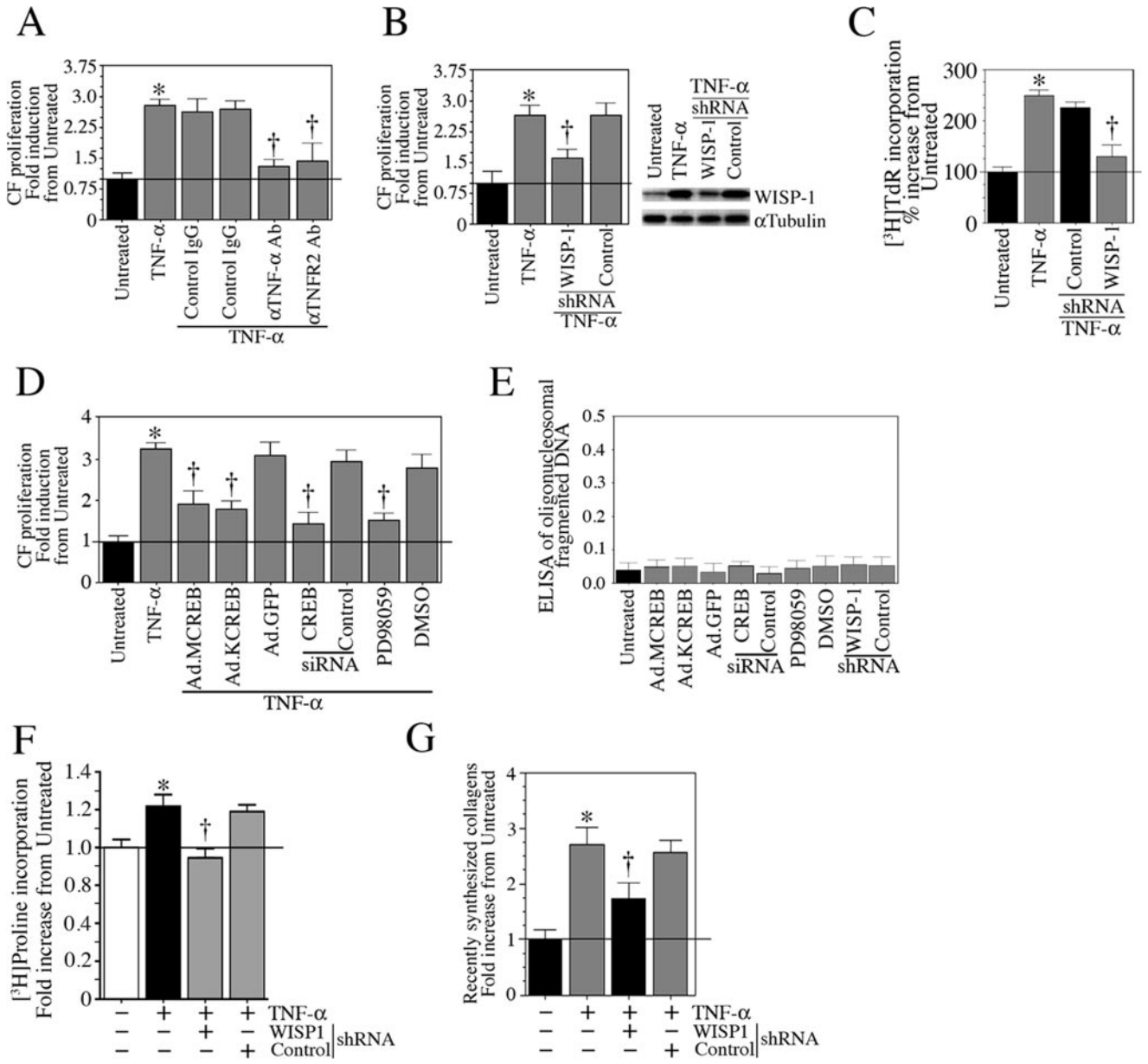


FIGURE 7. **TNF-α induces cardiac fibroblast proliferation and collagen synthesis via WISP1.** *A*, TNF-α stimulates CF proliferation. Quiescent CF were treated with TNF-α (10 ng/ml for 3 days), and CF proliferation was quantified by the CyQuant cell proliferation assay as described under "Experimental Procedures." Specificity of TNF-α was verified by preincubating cells with TNF-α- or TNFR2-neutralizing antibodies (*Ab*) (10 μg/ml for 1 h) before the addition of TNF-α. *, $p <$ 0.01 *versus* untreated; †, $p <$ at least 0.05 *versus* TNF-α ($n = 12$). *B* and *C*, TNF-α induces CF proliferation in part via WISP1. CF transfected with WISP1-specific or control shRNA expression vector were incubated with TNF-α for 3 days. Cell proliferation was quantified by CyQuant (*B*) and [$^3$H]TdR incorporation (*C*). Knockdown of WISP1 was confirmed by immunoblotting (*B*, *right panel*). *D*, TNF-α stimulates CF proliferation via ERK1/2 and CREB. CF treated as in Figs. 3*D* and 5*C* but were incubated with TNF-α for 3 days and then analyzed for proliferation by the CyQuant assay. *, $p < 0.001$ *versus* untreated; †, $p < 0.05$ *versus* TNF-α ($n = 12$). *E*, adenoviral transduction of mutant CREB, knockdown of CREB and WISP1, and treatment with PD failed to modulate CF viability. CF treated as in *D* were analyzed for cell death at 24 h by a cell death detection ELISA ($n = 12$). *F*, TNF-α stimulates collagen synthesis in a WISP1-dependent manner. CF transfected with WISP1-specific shRNA were incubated with TNF-α, and [$^3$H]proline incorporation was quantified as described under "Experimental Procedures," normalized to cell numbers, and represented as -fold increase from untreated. Specificity of TNF-α was verified by incubating cells with TNF-α-neutralizing antibodies before TNF-α addition. *, $p < 0.05$ *versus* untreated; †, $p < 0.05$ *versus* TNF-α + control shRNA ($n = 12$). *G*, TNF-α stimulates soluble collagen release in WISP1-dependent manner. CF transfected with WISP1-specific shRNA were incubated with TNF-α for 48 h. Recently synthesized collagens were quantified by Sircol Collagen assay, normalized to cell numbers, and represented as -fold increase from untreated. **, $p < 0.001$ *versus* untreated; †, $p <$ 0.01 *versus* TNF-α+control shRNA ($n = 12$).

of ECM proteins, including interstitial collagens, proteoglycans, and glycoproteins, which collectively provide structural support to myocardial constituent cells (46). Furthermore, the ECM also serves to bind the secreted cytokines, growth factors, and proteases, which not only influence fibroblast function but also transmit signals between fibroblasts and cardiomyocytes as well as between ECM and cardiomyocytes (46). ECM turnover in the heart under normal physiological conditions is a tightly regulated process. However, after insult or injury, the delicate balance between matrix metalloproteinases (MMPs) and their tissue inhibitors is altered in favor of the MMPs, resulting in enhanced

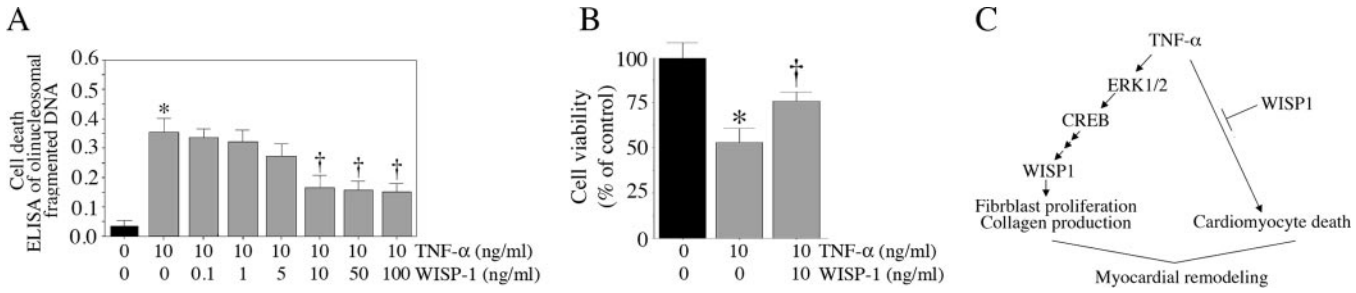


FIGURE 8. **WISP1 attenuates TNF-α-induced cardiomyocyte death.** *A*, WISP1 blocks TNF-α-induced cardiomyocyte death. NMVM were incubated with recombinant human WISP1 for 1 h before recombinant TNF-α (10 ng/ml for 24 h) addition. Cell death was analyzed by a cell death detection ELISA ($n = 12$). *, $p < 0.001$ *versus* untreated; †, $p < 0.01$ *versus* TNF-α. *B*, cell viability was also assessed by the MTT assay. NMVM treated as in *A* but with 10 ng/ml WISP1 were analyzed for cell viability using the MTT assay ($n = 12$). *, $p < 0.01$ *versus* untreated; †, $p < 0.01$ *versus* TNF-α. *C*, schema showing the signal transduction pathway involved in TNF-α-mediated WISP1 induction in cardiac fibroblasts, TNF-α-mediated WISP1-dependent fibroblast proliferation and collagen production, the pro-survival effects of WISP1 in TNF-α induced cardiomyocyte death, and the possible roles of TNF-α and WISP1 in post-infarct myocardial remodeling.

ECM degradation, fibroblast migration, proliferation, fibrosis, and pathological remodeling (46, 47).

Fibroblasts are the principal cell type responsible for fibrous tissue formation at the site of infarction (48). Although fibroblast-derived cytokines, growth factors and ECM proteins play a role in wound repair after injury or inflammation, they also actively participate in fibrosis and organogenesis (5, 6). Fibroblasts express various growth factors, including TGF-β and members of the CCN family, such as CTGF (5, 6). Although TGF-β and CTGF have been studied extensively, the expression, regulation, and roles of other CCN family members in cardiac pathophysiology are less well understood.

We have recently reported that myocardial infarction upregulates WISP1 expression (13). We have also shown that MI triggers the induction of biglycan, a small leucine-rich proteoglycan that binds WISP1 (13), suggesting that the elements for WISP1 signaling do exist in the post-infarction myocardium. We have also reported that TNF-α induces WISP1 expression in cardiomyocytes (13). Although induction of CCN family members by proinflammatory cytokines has already been reported, the novel observation of the present study is that treatment with TNF-α induces WISP1 expression in cardiac fibroblasts and that neither TNF-α, WISP1, nor a combination thereof induces fibroblast death. This is in contrast to what has been reported for other members of CCN family. Chen *et al.* (49) reported that although TNF-α alone is not cytotoxic, the presence of CCN1, CCN2, or CCN3 can unmask TNF-α cytotoxic effects and induce fibroblast death. These authors show that Cyr61 (CCN1) stimulates reactive oxygen species (ROS) generation via 5-lipoxygenase and the mitochondria through a RAC1-dependent pathway and suggest that the high and sustained levels of ROS induced by Cyr61/TNF-α result in the oxidative inactivation of JNK phosphatases, leading to persistent activation of JNK and subsequent cell death (49). In contrast to this observation, here we demonstrate that a combination of TNF-α and WISP1 induce fibroblast proliferation. Together, these studies suggest that members of the CCN family profoundly influence TNF-α signaling; although some unmask its cytotoxic effects, others such as WISP1 mediate its pro-mitogenic effects. In support of this hypothesis, we have previously reported that WISP1 potently activates the pro-survival factor Akt and Akt-dependent cardiomyocyte growth (13). Furthermore, WISP1 has been shown to attenuate p53-mediated apoptosis in response to DNA damage through activation of the Akt kinase (45).

Similar to their effects on TNF-α (44), members of the CCN family can also affect TGF-β. CTGF (CCN2) has been shown to modulate the bioavailability and signal transduction of TGF-β (50). CTGF physically interacts with TGF-β, enhancing binding to its receptors. Furthermore, knockdown of CTGF attenuates the expression of a subset of genes induced by TGF-β (47, 48), suggesting that TGF-β signals via both CTGF-dependent and -independent mechanisms. In addition, CTGF and TGF-β together induce a sustained pro-fibrotic response that is more effective than either factor alone (51). However, WISP1 has recently been shown to inhibit TGF-β-induced BrdUrd incorporation in osteoblasts, possibly via reduced Smad-2 phosphorylation (52). Whether WISP1 functions in a synergistic or antagonistic fashion with TGF-β in cardiac fibroblasts is presently under investigation.

Our results also show that TNF-α stimulates collagen synthesis in a WISP1-dependent manner. In fact, we have previously demonstrated that WISP1 is a potent inducer of collagen synthesis in fibroblasts (13), suggesting that TNF-α/WISP1 signaling exerts pro-fibrotic effects. Our data also show that TNF-α induces WISP1 expression in cardiac fibroblasts in a CREB-dependent manner. TNF-α induces CREB phosphorylation, DNA binding activity, and reporter gene induction. Furthermore, knockdown of CREB or overexpression of mutant CREB down-regulates TNF-α-mediated WISP1 induction, suggesting that CREB is a critical regulator of *WISP1* transcription. In support of this hypothesis, Xu *et al.* (27) have previously demonstrated that the *WISP1* 5′ *cis*-regulatory region contains binding sites for various transcription factors, including T-cell factor-lymphoid enhancer binding factor (TCF/LEF) and CREB. Although both TCF/LEF and CREB have been shown to play a role in β-catenin-induced *WISP1* transcription, mutation in the core CREB binding site, but not in TCF/LEF sites, significantly attenuate β-catenin-mediated *WISP1* transcription, suggesting that CREB plays an essential role in *WISP1* transcription.

CREB is a 43-kDa bZip nuclear transcription factor that is important in various cellular processes including cell death, proliferation, differentiation, memory, and glucose homeostasis (53). CREB regulates target gene transcription via binding to the CRE (cAMP response elements) as either a homodimer or a

heterodimer with other members of the CREB/activating transcription factor superfamily (53). Upon phosphorylation at Ser-133, phospho-CREB translocates to the nucleus and acts as a transcriptional activator. Phosphorylation at Ser-133 also facilitates the recruitment of the co-activator CREB-binding protein (CBP) and activates transcription (53).

CREB phosphorylation can be induced by diverse second messengers, such as phosphatidylinositol 3-kinase, Akt, protein kinase C, and ERK (53). In fact, our results showed that TNF-$\alpha$ induces CREB phosphorylation at Ser-133 via ERK1/2 activation, as evidenced by a significant inhibition in phospho-CREB levels when CF were pretreated with the MEK inhibitor U0126 or the ERK1/2 inhibitor PD98059, indicating that TNF-$\alpha$ induces CREB activation via MEK/ERK1/2-dependent signaling. Importantly, we also show that inhibition of CREB or ERK1/2 significantly blunts TNF-$\alpha$-induced CF proliferation, suggesting that ERK1/2-CREB signaling promotes fibroblast survival and proliferation. In support of this hypothesis, it has been demonstrated that norepinephrine stimulates cardiac fibroblast proliferation via CREB activation (54). Similarly, PDGF-BB mediates vascular smooth muscle cell proliferation via MEK-ERK1/2 and CREB activation (55). Activation of CREB also plays a role in angiotensin II-mediated smooth muscle cell hypertrophy (56). Furthermore, in cardiomyocyte hypoxia, insulin-like growth factor-1-induced antiapoptotic signaling was shown to require phosphatidylinositol 3-kinase and MEK/ERK1/2-dependent CREB activation (57). Enhanced CREB expression and its activation have also been shown to stimulate mitogenic signaling in tumor cells. Activation of CREB also induces the anti-apoptotic bcl-2 expression (58). However, in contrast to these observations, activation of CREB has been reported to suppress cell growth and proliferation. Activation of CREB can induce caspase-8 transcription and cell death in neuroblastoma cells (55) and can modulate the apoptotic threshold in cancer cells, inducing cell death by stimulating the expression of Smac (the second mitochondria-derived activator of caspases)/DIABLO (direct inhibitor of apoptosis proteins-binding protein with low isoelectric point) (59), a mitochondrial pro-apoptotic factor. Together, these reports indicate that, depending on the stimulus, cell type, and coactivators, activation of CREB can lead to either cell proliferation or death.

In this study we show that activation of CREB in CF promotes growth stimulatory effects, leading to TNF-$\alpha$-mediated WISP1 induction and WISP1-dependent fibroblast proliferation. The discovery that TNF-$\alpha$/WISP1 signaling stimulates collagen synthesis and fibroblast proliferation indicates a potential role for this pathway in post-MI cardiac remodeling and fibrosis.

One interesting observation in this study is that TNF-$\alpha$ induces WISP1 expression in a delayed manner. Although TNF-$\alpha$-dependent ERK1/2 and CREB activations occurred earlier, up-regulation in WISP1 expression was detected at 12 h, suggesting that either an intermediate factor induced by TNF-$\alpha$ or co-factors that influence CREB-mediated transcription might contribute to this delayed induction. In fact, our unpublished observations showed that TNF-$\alpha$ induces PDGF-B expression in fibroblasts. Because PDGF stimulates CREB phosphorylation and nuclear translocation (60), it is possible that TNF-$\alpha$-mediated PDGF-B might in part contribute to delayed WISP1 expression. We are expanding our studies by investigating the effects of TNF-$\alpha$ in cardiac fibroblasts by microarray analysis. It is also possible that the delay in CRE-mediated transcription could be because of the presence of inhibitors of CREB, which might dimerize with and inactivate CREB (61), or the presence of high levels of intracellular phosphatases that reverse CREB phosphorylation (62, 63). These inhibitors would need to be down-regulated before CREB can exert its effect. In addition, several additional factors might have contributed to delayed WISP1 induction in cardiac fibroblasts. For example, TNF-$\alpha$ is known to suppress TCF/LEF (64). Although TCF has been shown not to significantly alter WISP1 induction at basal levels (27), it might cooperate with CREB in enhancing WISP1 transcription. Furthermore, TNF-$\alpha$ is known to suppress intracellular levels of $\beta$-catenin (64), a key transducer of the Wnt signaling pathway. Thus, suppression of $\beta$-catenin might delay WISP1 transcription. Furthermore, suppressed nuclear $\beta$-catenin levels might reduce its interaction with the TCF/LEF and subsequent transcription of WISP1. Thus, TNF-$\alpha$ may stimulate activation and cross-talk of multiple signal transduction pathways and, thus, play an important role in regulating WISP1 transcription. Studies are in progress to unravel these interactions.

TNF-$\alpha$ is also known to potently activate NF-$\kappa$B in various cell types, and the ability of TNF-$\alpha$ to regulate cellular gene expression in most instances is attributed to activation of NF-$\kappa$B-dependent signaling. Results in the present study show that, indeed, TNF-$\alpha$ activates NF-$\kappa$B, and although its inhibition attenuates $\kappa$B-responsive MMP9 expression, the expression of WISP1 is not significantly modulated. Furthermore, no potential/putative $\kappa$B binding site(s) was identified in WISP1 5′-untranslated region (~2 kilobases from transcription start site). However, we do not rule out the possibility that NF-$\kappa$B activation might influence WISP1 expression in a cell type- and stimulus-specific manner by cooperating or competing with the CREB co-activator CREB-binding protein (65). Together, our studies suggest that NF-$\kappa$B, although activated, is not a significant modulator of WISP1 expression in TNF-$\alpha$-treated CF.

Another critical observation in the present study is that WISP1 exerts pro-survival effects in cardiomyocytes. Although TNF-$\alpha$ induces significant cardiomyocyte death, pretreatment with WISP1 antagonizes TNF-$\alpha$ cytotoxicity, indicating that WISP1 exerts diverse biological effects (*e.g.* pro-survival, pro-mitogenic, and pro-hypertrophic) within the heart in a cell type-specific manner. Because TNF-$\alpha$ has been reported to induce cardiomyocyte death via p38MAPK activation, inhibition of bcl-2, and an increasing Bax to bcl-xl (B cell leukemia-x long) ratio (66), we hypothesize that treatment with WISP1 will reverse this phenomenon, promoting cardiomyocyte survival. Studies are under way to address this possibility.

In summary, our results demonstrate that both TNF-$\alpha$ and WISP1 are up-regulated in the myocardium post-infarct and that WISP1 significantly modulates TNF-$\alpha$ effects in cardiac cell type specific manner, mediating TNF-$\alpha$-induced fibroblast proliferation and attenuating TNF-$\alpha$-induced cardiomyocyte death. Because TNF-$\alpha$ and WISP1 are up-regulated in the myocardium post-infarct, our results indicate that a TNF-$\alpha$/WISP1 signaling may contribute to post-infarct cardiac remodeling.

## REFERENCES


1. Tiyyagura, S. R., and Pinney, S. P. (2006) *Mt. Sinai J. Med.* **73,** 840–851
2. Pfeffer, M. A., and Braunwald, E. (1990) *Circulation* **81,** 1161–1172
3. Kurrelmeyer, K., Kalra, D., Bozkurt, B., Wang, F., Dibbs, Z., Seta, Y., Baumgarten, G., Engle, D., Sivasubramanian, N., and Mann, D. L. (1998) *Clin. Cardiol.* **21,** 14–19
4. Munoz, V., Campbell, K., and Shibayama, J. (2008) *J. Physiol.* (*Lond.*) **586,** 2423–2424
5. Banerjee, I., Yekkala, K., Borg, T. K., and Baudino, T. A. (2006) *Ann. N. Y. Acad. Sci.* **1080,** 76–84
6. Baudino, T. A., Carver, W., Giles, W., and Borg, T. K. (2006) *Am. J. Physiol. Heart Circ. Physiol.* **291,** 1015–1026
7. Reddy, V. S., Harskamp, R. E., van Ginkel, M. W., Calhoon, J., Baisden, C. E., Kim, I. S., Valente, A. J., and Chandrasekar, B. (2008) *J. Cell. Physiol.* **215,** 697–707
8. Colston, J. T., Chandrasekar, B., and Freeman, G. L. (2002) *J. Biol. Chem.* **277,** 23477–23483
9. Venkatachalam, K., Mummidi, S., Cortez, D. M., Prabhu, S. D., Valente, A. J., and Chandrasekar, B. (2008) *Am. J. Physiol. Heart Circ. Physiol.* **294,** 2078–2087
10. Chen, C. C., and Lau, L. F. (2009) *Int. J. Biochem. Cell Biol.* **41,** 771–783
11. Yeger, H., and Perbal, B. (2007) *J. Cell Commun. Signal.* **1,** 159–164
12. Shi-Wen, X., Leask, A., and Abraham, D. (2008) *Cytokine Growth Factor Rev.* **19,** 133–144
13. Colston, J. T., de la Rosa, S. D., Koehler, M., Gonzales, K., Mestril, R., Freeman, G. L., Bailey, S. R., and Chandrasekar, B. (2007) *Am. J. Physiol. Heart Circ. Physiol.* **293,** 1839–1846
14. Haudek, S. B., Taffet, G. E., Schneider, M. D., and Mann, D. L. (2007) *J. Clin. Investig.* **117,** 2692–2701
15. Diwan, A., Dibbs, Z., Nemoto, S., DeFreitas, G., Carabello, B. A., Sivasubramanian, N., Wilson, E. M., Spinale, F. G., and Mann, D. L. (2004) *Circulation* **109,** 262–268
16. Nakano, M., Knowlton, A. A., Dibbs, Z., and Mann, D. L. (1998) *Circulation* **97,** 1392–1400
17. Kurrelmeyer, K. M., Michael, L. H., Baumgarten, G., Taffet, G. E., Peschon, J. J., Sivasubramanian, N., Entman, M. L., and Mann, D. L. (2000) *Proc. Natl. Acad. Sci. U. S. A.* **97,** 5456–5461
18. Bradley, J. R. (2008) *J. Pathol.* **214,** 149–160
19. Anker, S. D., and von Haehling, S. (2004) *Heart* **90,** 464–470
20. Patel, D. N., King, C. A., Bailey, S. R., Holt, J. W., Venkatachalam, K., Agrawal, A., Valente, A. J., and Chandrasekar, B. (2007) *J. Biol. Chem.* **282,** 27229–27238
21. Chandrasekar, B., Mummidi, S., Mahimainathan, L., Patel, D. N., Bailey, S. R., Imam, S. Z., Greene, W. C., and Valente, A. J. (2006) *J. Biol. Chem.* **281,** 15099–15109
22. Council, N. R. (1996) *Guide for the Care and Use of Laboratory Animals*, National Academy Press, Washington, DC
23. Chandrasekar, B., Mitchell, D. H., Colston, J. T., and Freeman, G. L. (1999) *Circulation* **99,** 427–433
24. Cortez, D. M., Feldman, M. D., Mummidi, S., Valente, A. J., Steffensen, B., Vincenti, M., Barnes, J. L., and Chandrasekar, B. (2007) *Am. J. Physiol. Heart Circ. Physiol.* **293,** 3356–3365
25. Sarkar, S. A., Gunter, J., Bouchard, R., Reusch, J. E., Wiseman, A., Gill, R. G., Hutton, J. C., and Pugazhenthi, S. (2007) *Diabetologia* **50,** 1649–1659
26. Chandrasekar, B., Patel, D. N., Mummidi, S., Kim, J. W., Clark, R. A., and Valente, A. J. (2008) *J. Biol. Chem.* **283,** 4200–4209
27. Xu, L., Corcoran, R. B., Welsh, J. W., Pennica, D., and Levine, A. J. (2000) *Genes Dev.* **14,** 585–595
28. Chandrasekar, B., Streitman, J. E., Colston, J. T., and Freeman, G. L. (1998) *Biochim. Biophys. Acta* **1406,** 91–106
29. Colston, J. T., de la Rosa, S. D., and Freeman, G. L. (2004) *Biochem. Biophys. Res. Commun.* **316,** 256–262
30. Junquiera, L. C., Junqueira, L. C., and Brentani, R. R. (1979) *Anal. Biochem.* **94,** 96–99
31. Liu, X., Sun, S. Q., Hassid, A., and Ostrom, R. S. (2006) *Mol. Pharmacol.* **70,** 1992–2003
32. Chandrasekar, B., Mummidi, S., Claycomb, W. C., Mestril, R., and Nemer, M. (2005) *J. Biol. Chem.* **280,** 4553–4567
33. Irwin, M. W., Mak, S., Mann, D. L., Qu, R., Penninger, J. M., Yan, A., Dawood, F., Wen, W. H., Shou, Z., and Liu, P. (1999) *Circulation* **99,** 1492–1498
34. Nian, M., Lee, P., Khaper, N., and Liu, P. (2004) *Circ. Res.* **94,** 1543–1553
35. Hirschl, M. M., Gwechenberger, M., Binder, T., Binder, M., Graf, S., Stefenelli, T., Rauscha, F., Laggner, A. N., and Sochor, H. (1996) *Eur. Heart J.* **17,** 1852–1859
36. Vaddi, K., Nicolini, F. A., Mehta, P., and Mehta, J. L. (1994) *Circulation* **90,** 694–699
37. Frangogiannis, N. G., Smith, C. W., and Entman, M. L. (2002) *Cardiovasc. Res.* **53,** 31–47
38. Jacobs, M., Staufenberger, S., Gergs, U., Meuter, K., Brandstatter, K., Hafner, M., Ertl, G., and Schorb, W. (1999) *J. Mol. Cell. Cardiol.* **31,** 1949–1959
39. Porter, K. E., Turner, N. A., O'Regan, D. J., and Ball, S. G. (2004) *Cardiovasc. Res.* **64,** 507–515
40. Ono, H., Ichiki, T., Fukuyama, K., Iino, N., Masuda, S., Egashira, K., and Takeshita, A. (2004) *Arterioscler. Thromb. Vasc. Biol.* **24,** 1634–1639
41. Gustin, J. A., Pincheira, R., Mayo, L. D., Ozes, O. N., Kessler, K. M., Baerwald, M. R., Korgaonkar, C. K., and Donner, D. B. (2004) *Am. J. Physiol. Cell Physiol.* **286,** 547–555
42. Gonzalez, G. A., Menzel, P., Leonard, J., Fischer, W. H., and Montminy, M. R. (1991) *Mol. Cell. Biol.* **11,** 1306–1312
43. Clerk, A., Harrison, J. G., Long, C. S., and Sugden, P. H. (1999) *J. Mol. Cell. Cardiol.* **31,** 2087–2099
44. Chen, G., and Goeddel, D. V. (2002) *Science* **296,** 1634–1635
45. Su, F., Overholtzer, M., Besser, D., and Levine, A. J. (2002) *Genes Dev.* **16,** 46–57
46. Sun, Y. (2009) *Cardiovasc. Res.* **81,** 482–490
47. Wynn, T. A. (2008) *J. Pathol.* **214,** 199–210
48. Powell, D. W., Mifflin, R. C., Valentich, J. D., Crowe, S. E., Saada, J. I., and West, A. B. (1999) *Am. J. Physiol. Cell Physiol.* **277,** 1–9
49. Chen, C. C., Young, J. L., Monzon, R. I., Chen, N., Todorovic, V., and Lau, L. F. (2007) *EMBO J.* **26,** 1257–1267
50. Abreu, J. G., Ketpura, N. I., Reversade, B., and De Robertis, E. M. (2002) *Nat. Cell Biol.* **4,** 599–604
51. Mori, T., Kawara, S., Shinozaki, M., Hayashi, N., Kakinuma, T., Igarashi, A., Takigawa, M., Nakanishi, T., and Takehara, K. (1999) *J. Cell. Physiol.* **181,** 153–159
52. Inkson, C. A., Ono, M., Kuznetsov, S. A., Fisher, L. W., Robey, P. G., and Young, M. F. (2008) *J. Cell. Biochem.* **104,** 1865–1878
53. Mayr, B., and Montminy, M. (2001) *Nat. Rev. Mol. Cell Biol.* **2,** 599–609
54. Leicht, M., Greipel, N., and Zimmer, H. (2000) *Cardiovasc. Res.* **48,** 274–284
55. Jiang, L. P., Lu, Y., Nie, B. M., and Chen, H. Z. (2008) *Chem. Biol. Interact.* **171,** 348–354
56. Funakoshi, Y., Ichiki, T., Takeda, K., Tokuno, T., Iino, N., and Takeshita, A. (2002) *J. Biol. Chem.* **277,** 18710–18717
57. Mehrhof, F. B., Muller, F. U., Bergmann, M. W., Li, P., Wang, Y., Schmitz, W., Dietz, R., and von Harsdorf, R. (2001) *Circulation* **104,** 2088–2094
58. Pugazhenthi, S., Nesterova, A., Sable, C., Heidenreich, K. A., Boxer, L. M., Heasley, L. E., and Reusch, J. E. (2000) *J. Biol. Chem.* **275,** 10761–10766
59. Martinez-Velazquez, M., Melendez-Zajgla, J., and Maldonado, V. (2007) *Cell. Signal.* **19,** 1212–1220
60. Seternes, O. M., Johansen, B., and Moens, U. (1999) *Mol. Endocrinol.* **13,** 1071–1083
61. Sassone-Corsi, P. (1995) *Annu. Rev. Cell Dev. Biol.* **11,** 355–377
62. Bito, H., Deisseroth, K., and Tsien, R. W. (1996) *Cell* **87,** 1203–1214
63. Liu, F. C., and Graybiel, A. M. (1996) *Neuron* **17,** 1133–1144
64. Lee, E. O., Shin, Y. J., and Chong, Y. H. (2004) *J. Neuroimmunol.* **155,** 21–31
65. Zhong, H., Voll, R. E., and Ghosh, S. (1998) *Mol. Cell* **1,** 661–671
66. Dhingra, S., Sharma, A. K., Singla, D. K., and Singal, P. K. (2007) *Am. J. Physiol. Heart Circ. Physiol.* **293,** 3524–3531